Dalton Transactions

Accepted Manuscript

This article can be cited before page numbers have been issued, to do this please use: A. Uslu, S. O. Tümay, A. enocak, F. Yuksel, E. Özcan and S. Yeilot, *Dalton Trans.*, 2017, DOI: 10.1039/C7DT01134B.

This is an Accepted Manuscript, which has been through the Royal Society of Chemistry peer review process and has been accepted for publication.

Accepted Manuscripts are published online shortly after acceptance, before technical editing, formatting and proof reading. Using this free service, authors can make their results available to the community, in citable form, before we publish the edited article. We will replace this Accepted Manuscript with the edited and formatted Advance Article as soon as it is available.

You can find more information about Accepted Manuscripts in the author guidelines.

Please note that technical editing may introduce minor changes to the text and/or graphics, which may alter content. The journal's standard Terms & Conditions and the ethical guidelines, outlined in our author and reviewer resource centre, still apply. In no event shall the Royal Society of Chemistry be held responsible for any errors or omissions in this Accepted Manuscript or any consequences arising from the use of any information it contains.

ROYAL SOCIETY OF CHEMISTRY

rsc.li/dalton

View Article Online
DOI: 10.1039/C7DT01134B

Imidazole/Benzimidazole-Modified Cyclotriphosphazenes as Highly Selective Fluorescent Probes for Cu^{2+}: Synthesis, Configurational Isomers, and Crystal Structures

Aylin Uslu*, Süreyya Oğuz Tümay, Ahmet Şenocak, Fatma Yuksel, Elif Özcan, Serkan Yeşilot*

Department of Chemistry, Gebze Technical University, Gebze 41400, Kocaeli, Turkey

∗ Corresponding authors. Tel.: +90 262 6053009 and +90 262 6053014
E-mail addresses: aylin@gtu.edu.tr and yesil@gtu.edu.tr

keywords: Fluorescent probe, copper, imidazole, benzimidazole, phosphazene

ABSTRACT

Configurational isomers (*cis*- and *trans*) of imidazole- or benzimidazole-modified cyclotriphosphazenes (**3a**,**4a** or **3b, 4b**) were designed, synthesized and investigated as fluorescent probes for metal ions. The newly synthesized compounds were characterized by ^{1}H and ^{31}P NMR; and MALDI MS spectrometry. The configurations of geometric isomers were analyzed by X-ray crystallography and ^{31}P NMR spectroscopy on addition of CSA. The photophysical behaviour and metal ion selectivity of compounds were investigated by UV/vis and fluorescence spectroscopies. Among the examined 20 metal ions, the fluorescence emission of the isomer mixtures were quenched by Cu^{+2} together with Fe^{2+}, Fe^{3+}, Zn^{2+} and Ni^{2+} ions, but each individual isomer (**3a**,**b** and **4a**,**b**) exhibited on-off-type fluorescence response with high selectivity towards only Cu^{2+} with the low limits of detection ranging from 1.27 μM to 2.04 μM. The complex stoichiometries of **3a**,**b** and **4a**,**b** with Cu^{2+} were determined as 1:1 (L/M) using the method of continuous variation (Job's plot) and density functional theory (DFT) calculation, moreover the complex formation of **4a** with Cu^{2+} was unambiguously determined by X-ray crystallographic analysis that is consistent with the results obtained by the Job's plots as well as DFT.

View Article Online
DOI: 10.1039/C7DT01134B

1. Introduction

Transition-metal ions can cause important environmental and health problems because of their toxicity.[1] Among these metal ions, as one of the most abundant transition-metal ions with zinc and iron, copper plays a significant role in many fundamental biological and environmental processes.[2] However, excessive copper content in body can cause serious health problem like liver or kidney damage and high levels of copper is also seriously toxic to environment.[3-5] Copper contamination is still a challenging problem for today and future due to common use of copper in agriculture and industry. Moreover, maximum acceptable level of copper in water has been settled 1.3 mg/L (nearly 20μM/L) and 2.0 mg/L (nearly 30μM/L) by U.S. Environmental Protection Agency (EPA) and the World Health Organization (WHO), respectively.[6,7] Therefore, in past two decades, development of highly sensitive, selective and simple analytical methods for the detection of Cu^{2+}, especially for the trace amounts, in human body and environment have attracted great attention.[8-12] Compared to conventional analytical methods, such as high performance liquid chromatography, mass spectrometry and atomic absorption spectroscopy, fluorescent probes have received increasing attention due to their advantages including high sensitivity, low cost, short response time and easy operation and useful applications in the chemistry, biology and environment.[13-17] Numerous fluorescence probes exist about Cu^{2+} detecting but many of these are lack of selectivity and have relatively high detection limits.[18-22] So, the research and development of synthesis some highly sensitive and selective fluorescent probes for the detection of Cu^{2+} have emerged as an important task in the field of chemical probes in recent years.[18-25]

There is great interest in imidazole/benzimidazole ligands for structural chemistry because they are very functional fluorophores to develop fluorescent probes. Although the unsubstituted imidazole/benzimidazole have been known for their strong ability to bind with many metal ions, their chemically modified derivatives could be employed as highly selective fluorescent probes for the detecting different metal ions selectively such as Fe^{3+},[26-29] Cr^{3+},[26] Al^{3+},[30] Zn^{2+},[31,32] Ag^{+} [33] and Cu^{2+}.[8,9,11,34-36] In recent years, there has been considerable interest in preparation of fluorescent probes containing cyclophosphazene cores[37-43] due to having hard inorganic rings containing six or eight halogen atoms that can be easily modified by nucleophilic reaction with the desired groups.[44] Furthermore, chlorocyclophosphazenes are optically inert and their physical and chemical properties can be tailored by the choice of appropriate substituted groups on phosphorus atoms. At the same

View Article Online
DOI: 10.1039/C7DT01134B

time cyclophosphophosphazenes have the ability to engage in coordination to transition metals by different pendant donor groups attached the phosphazene skeleton and phosphazene systems possessing nitrogens on the site groups have been prepared that demonstrate coordination modes using various combinations of nitrogens of ring and/or site groups.[45-47] For example, the geminal, non-geminal, tetra- or hexasubstituted pyrazolyl, pyridyloxy, or pyridylamino-cyclophosphazene ligands have been extensively examined by the known regio- and stereo-selectivities involved in the nucleophilic substitution reactions of chlorocyclophosphazenes for the potential to bind many metal ions.[48,49] Specifically, it was found that the pyrazolyl-substituted cyclophosphazene ligands were very suitable and stable to form complex with the copper ions.[50-52] Inspired by the previously reported with a well-defined copper complex based on pyrazolyl-substituted cyclophosphazenes, we decided to exploit a similar approach to choose the imidazole or benzimidozole groups as the functional fluorophores which are the analogues to a pyrazole with two adjacent nitrogen atoms for design of new fluorescent copper probes. To the best of our knowledge, however, no isolated configurational isomers of phosphazene-based fluorescent probe for selective detection of Cu^{2+} has been reported so far.

In the present study, firstly phenyl and phenol groups were attached to cyclotriphosphazene core in a non-geminal position in order to generate the configurational isomers. Then, the imidazole or benzimidazole groups were modified with cyclotriphosphazene core in the non-geminal position to synthesize some efficient compounds possessing appropriate binding sites for transition metal ions to investigate their metal detecting abilities. We have also desired to obtain both of the configurational isomers (*cis*/*trans*) of these compounds in pure form, so as to able to examine their metal detecting abilities individually. All synthesized ligands were characterized by the usual spectroscopic and spectrometric techniques as well as elucidated their stereogenic properties by X-ray crystallography and ^{31}P NMR spectroscopy in the presence of a chiral solvating agent (CSA). X-ray crystallography was also used for determining the structure of ligand-Cu^{2+} complex that could be obtained as a crystal.

2. Results and discussion

2.1. Syntheses and characterization

In this work, some fluorescent efficient *cis* and *trans* isomers containing azole side groups were designed and synthesized using cyclotriphosphazene as a core in order to investigate their metal detecting abilities as fluorescent probes. Imidazole or benzimidazole groups were

View Article Online
DOI: 10.1039/C7DT01134B

non-geminally substituted into phosphazene ring to generate the potential metal binding site because metal binding takes place mostly between nitrogen atoms of non-geminally substitutens.[45,47] Newly synthesized compounds were characterized using mass, ^{31}P and ^{1}H NMR spectroscopies and X-ray crystallography. The mass, ^{31}P and ^{1}H NMR spectra data of all the compounds were given in supporting information.

Designed molecules were constructed by a stepwise synthesis. For this purpose, firstly compound **1,** 2,2,4,4-tetrachloro-6,6-diphenylcyclotriphosphazene [$N_3P_3Cl_4(Ph)_2$], was prepared as described in the literature.[53] Then, the compound **1** was reacted with phenol in 1:2 ratio in THF and presence of sodium hydride for eight hours at room temperature as shown in Scheme 1. It is known that phenoxy reagent was substituted to cyclophosphazene ring via a non-geminal pathway that generates stable configurational diastereoisomers as *cis* and *trans*.[53] The proton decoupled ^{31}P NMR spectrum of the reaction mixture which was given in Figure 1a showed the formation of two main products which can be referred to as configurational isomers as expected. From this reaction, a small quantity of pure **2a** and a mixture of two main products (**2a** and **2b**, Scheme 1) could be isolated. However, the compound **2b** couldn't be isolated in pure form and after that the mixture of **2a** and **2b** was used for subsequent reactions.

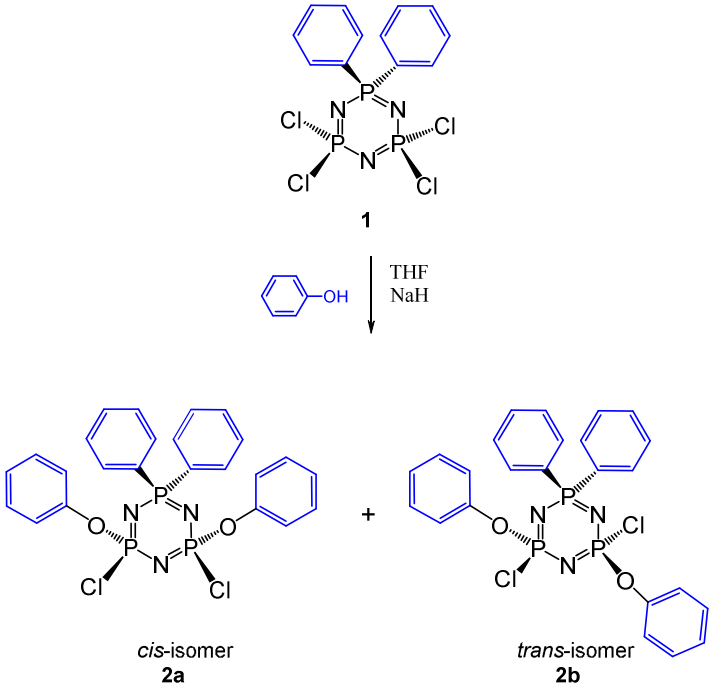

Scheme 1. The reaction of compound **1** with phenol to give the *cis* and *trans* mixture of compounds **2a** and **2b**.

View Article Online
DOI: 10.1039/C7DT01134B

The proton decoupled ^{31}P NMR spectrum of the reaction mixture which was given in Figure 1a showed two AX_2 spin systems that leads likely the *cis–trans* configurational isomers and the proton decoupled ^{31}P NMR spectrum of **2a** in Figure 1b was analyzed as AX_2 spin system. The relative amounts of the products found from the ^{31}P NMR spectrum of the reaction mixture (Figure 1a) were 45% and 55% for **2a** and **2b**, respectively. The crystal structure of compound **2a** was reported in this work and it was later confirmed that the configuration of the compound **2a** was the *cis* isomer.

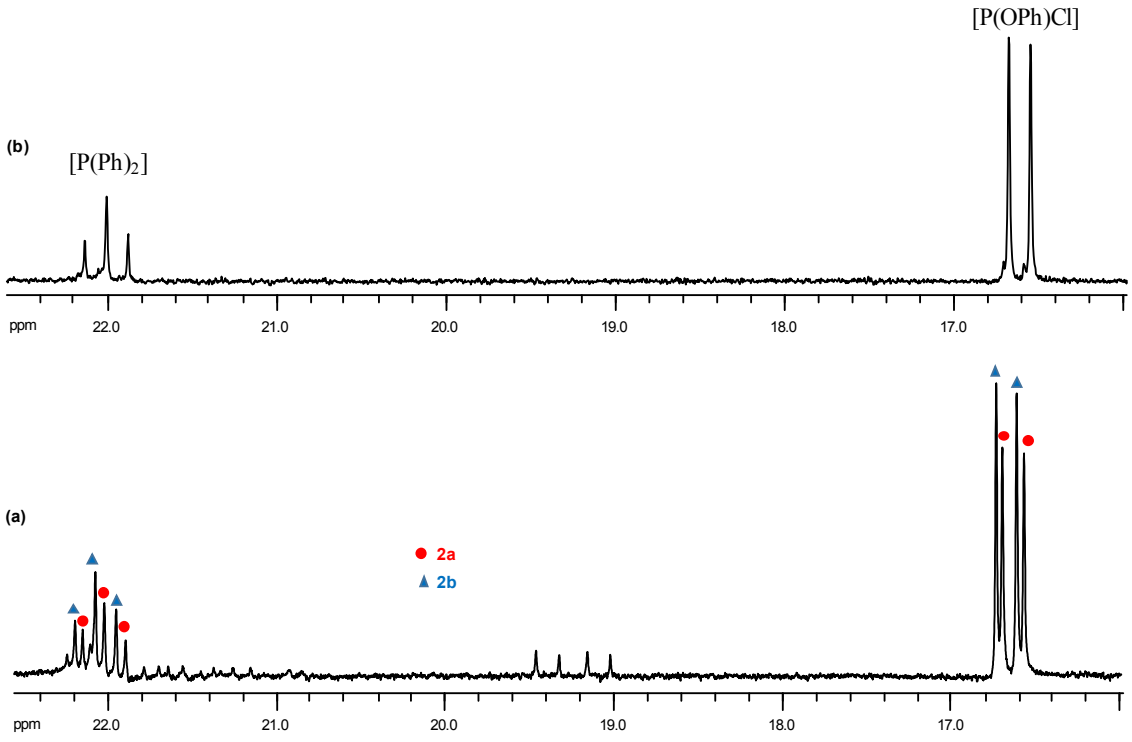

Figure 1. The proton decoupled ^{31}P NMR spectra of (a) the reaction mixture of phenol with $N_3P_3Cl_4(Ph)_2$ and (b) compound **2a**.

Compounds **3a**,**b** and **4a**,**b** were obtained as pure form from the reactions of mixture of **2a**,**b** with imidazole and benzimidazole, respectively. The substitution reactions were carried out according to Scheme 2. When the mixture of compounds **2a** and **2b** was treated with each azole group in a 1:2 molar ratio refluxing in THF and in the presence of triethylamine, the non-geminal diphenol di-azole compounds, **3a,b** or **4a,b** were obtained as shown in Scheme 2.

View Article Online
DOI: 10.1039/C7DT01134B

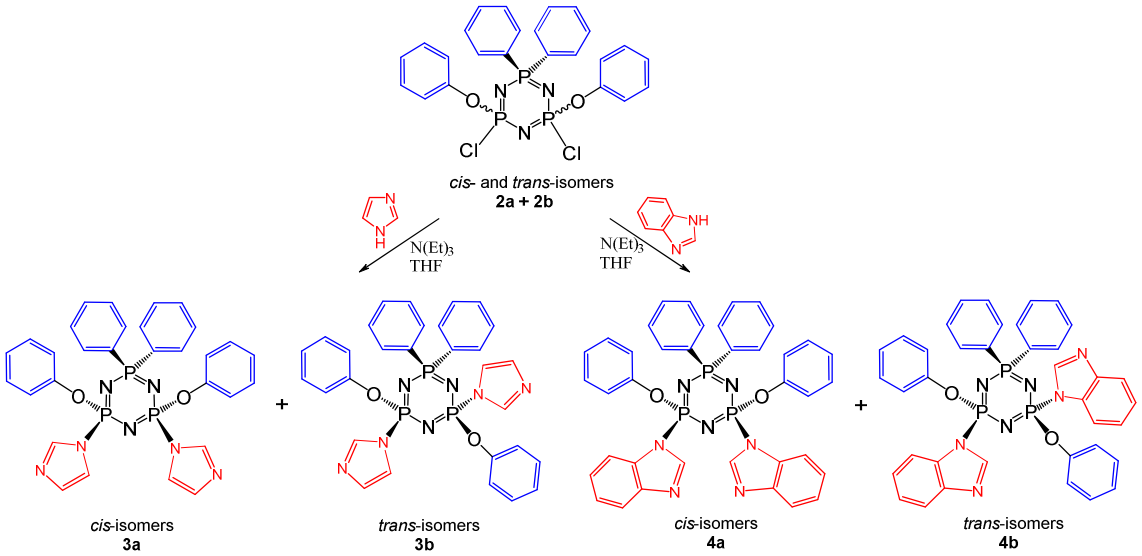

Scheme 2. The reactions of the mixture of compounds **2a** and **2b** with imidazole and benzimidazole to give compounds **3a,b** and **4a,b**, respectively.

The formation of two main products (**3a** and **3b**) which were isolated as pure from the reaction mixture were observed as AX_2 spin systems in the proton decoupled ^{31}P NMR spectrum of reaction mixture of **2a**,**b** with imidazole that was indicative of complete replacement of chlorine atoms by the azole groups. The relative amounts of each product determined from this ^{31}P NMR spectrum were about 36% and 64% for **3a** and **3b**, respectively. The proton-decoupled ^{31}P NMR spectra of pure compounds **3a** and **3b** were observed as AX_2 spin systems. X-ray crystallography later confirmed that compounds **3a** and **3b** were the *cis* and *trans* compounds, respectively.

The same case also occurred for isomers **4a** and **4b** that the reaction mixture spectrum was analyzed as two AX_2 spin systems. The proton-decoupled ^{31}P NMR spectra of reaction mixture and isolated compounds **4a**, **4b** from this mixture were given in Figure 2 as an example. The relative proportions observed from the spectrum were 45% and 55% for **4a** and **4b**, respectively, as shown in Figure 2a. The phosphorus chemical shifts, phosphorus-phosphorus coupling constants of all synthesized compounds were summarized in Table 4.

View Article Online
DOI: 10.1039/C7DT01134B

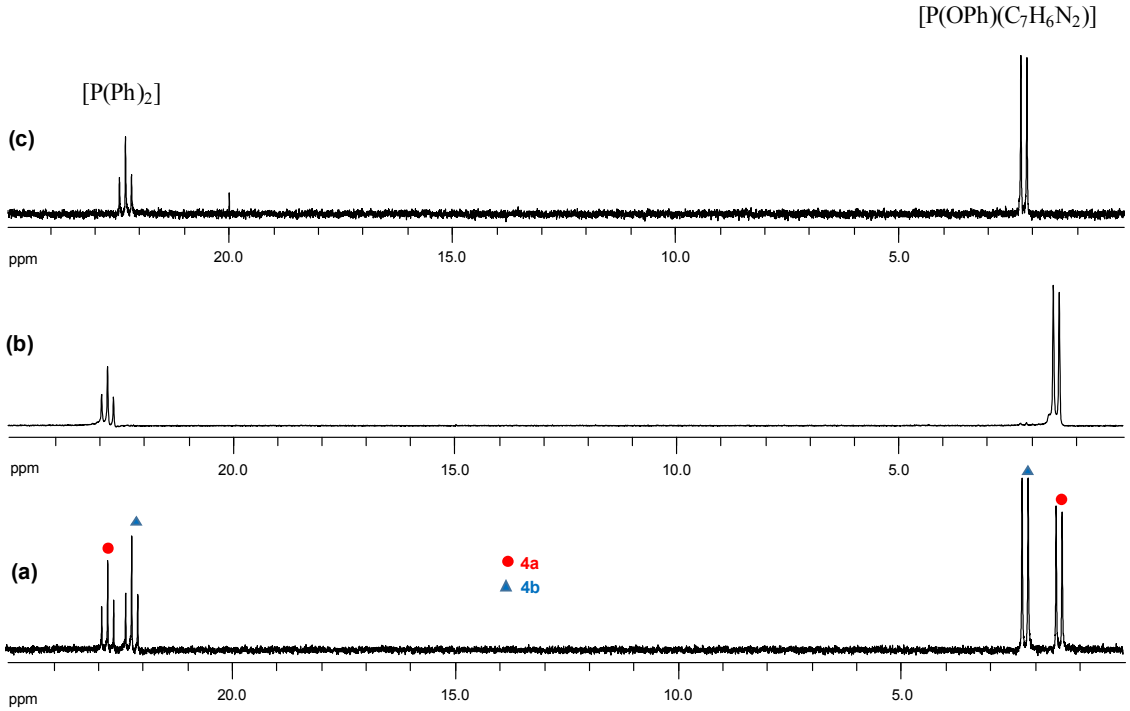

Figure 2. The proton decoupled ^{31}P NMR spectra of (a) the reaction mixture of benzimidazole with the mixture of **2a**,**b**; (b) compound **4a** and (c) compound **4**b.

The complexation reactions of obtained ligands **3a**,**b** and **4a**,**b** with Cu(II) were done in order to understand the correlation between the structure and complexation and only Cu(II) complex of **4a** was obtained as X-ray suitable pale blue crystals (compound **5**).

2.2. Crystal structure analysis

The molecular structures of six compounds, **2a, 3a, 3b, 4a, 4b** and **5** were established by single crystal x-ray structural analysis and the selected crystallographic data and refinement parameters were presented in Table 1. All structures were cyclotriphosphazene derivatives containing six-membered P_3N_3 ring and their crystal structures confirmed the assignments from those spectroscopic data as shown in Figures 3-6. The six-membered cyclotriphosphazene (P_3N_3) ring was geminal di-substituted with phenyl- (Ph) and non-geminal di-substituted with phenoxy- (PhO) in compound **2a** (Figure 3). Two PhO- groups of compound **2a** were in the same side of phosphazene ring to produce *cis* configuration. The substitution of the mixture of compounds **2a** and **2b** with two imidazole (im-) or benzimidazole (bim-) units, respectively gave geometrical isomers, **3a,b** (Figure 4) and **4a,b**

View Article Online
DOI: 10.1039/C7DT01134B

(Figure 5) in which two PhO- groups and two imidazole or benzimidazole groups were either on the same or opposite sides of phosphazene rings to produce *cis* or *trans* configurations.

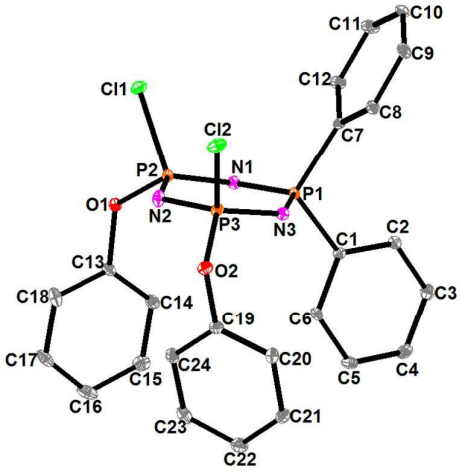

Figure 3. View of the molecular structure for compound **2a** with the atom-numbering scheme. Displacement ellipsoids are drawn at the 30% probability level. The hydrogen atoms have been omitted for clarity.

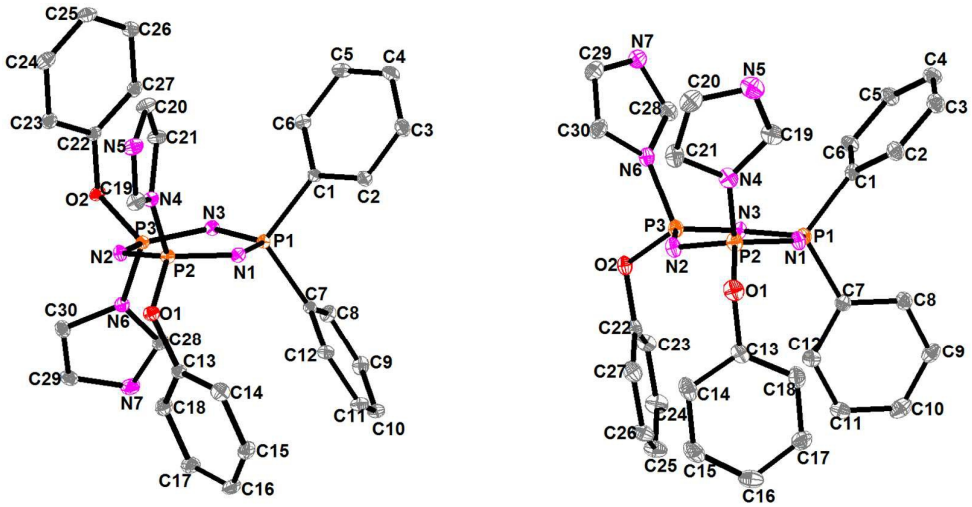

a) **b)**

Figure 4. Views of the molecular structures of **(a)** compound **3a** and **(b)** compound **3b** with the atom numbering scheme. Displacement ellipsoids are drawn at the 30% probability level. The hydrogen atoms have been omitted for clarity.

View Article Online
DOI: 10.1039/C7DT01134B

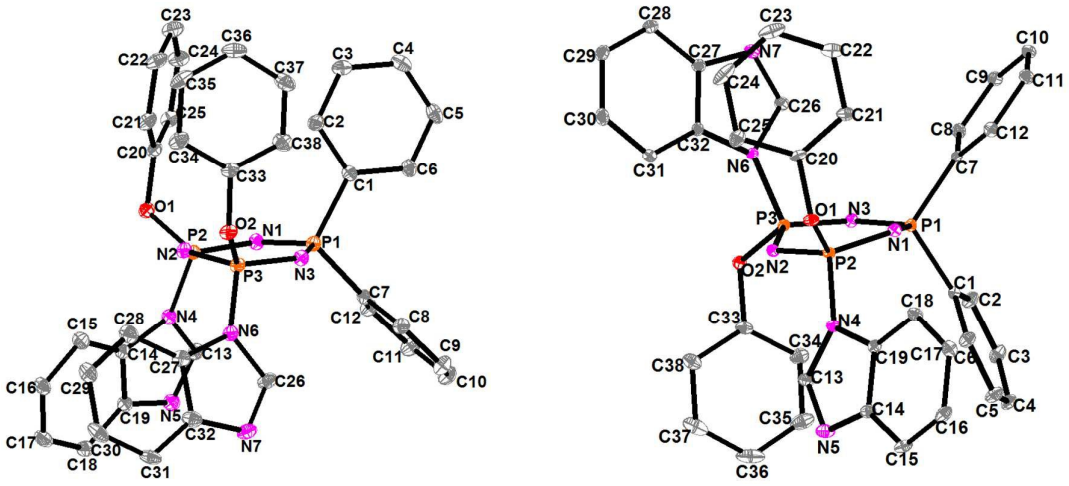

a) **b)**

Figure 5. Views of the molecular structures of **(a)** compound **4a** and **(b)** compound **4b** with the atom numbering scheme. Displacement ellipsoids are drawn at the 30% probability level. The hydrogen atoms have been omitted for clarity.

The conformational parameters of cyclotriphosphazene rings of studied compounds were presented in Table 2. The cyclophosphazene ring has a flattened chair conformation in compounds **2a** and **3a** while it has a flattened boat conformation in compounds **3b**, **4a** and **4b**. The maximum deviation from the plane of the cyclophosphazene ring in compound **2a** was 0.0785 (12) Å (on P2 atom). The substitutions with either imidazole or benzimidazole groups caused to increase on maximum deviation from planarity in compounds **3a,b** and **4a,b**. The deviation from planarity of phosphazene ring was larger in benzimidazole substituted derivatives **4a,b** then imidazole substituted derivatives **3a**,**b**; it was 0.1065(16)Å (on P3) for **3a** and 0.1018(16)Å (on N3) for **3b** while it was 0.1177(13)Å (on P2) for **4a** and 0.1487 (15) (on N1) Å **4b** (Table 2). The most deviation was observed in binuclear copper complex compound **5** in which the max. deviation from planarity was 0.181(4) Å (on P2 atom).

The selected bond parameters of the compounds **2a, 3a,b, 4a,b**, and **5** were summarized in Table 2. The substituent effect on P-N bond parameters was observed: the P-N bond lengths involving the gem-diphenyl substituted P1 phosphorus atom [$P(Ph)_2$] were longer than other P-N bond lengths involving the P2 and P3 phosphorus atoms which were non-gem-substituted with phenoxy and chlorine, imidazole or benzimidazole groups

View Article Online
DOI: 10.1039/C7DT01134B

[P(PhO)Cl, P(PhO)(im) and P(PhO)(bim)], because the electron-donating substituents increase the adjacent P-N bond lengths.[54]

The N–P–N bond angle belong to P1 phosphorus atom [$P(Ph)_2$] was smaller than those observed for P2 and P3 phosphorus atoms in all compounds. On the contrary, the endocyclic P–N–P bond angles of N2 nitrogen atom present between P2 and P3 phosphorus atoms [P(PhO)Cl, P(PhO)(im) and P(PhO)(bim)] was smallest. All these systematic differences observed between $P(Ph)_2$ and other P(PhO)Cl, P(PhO)(im) or P(PhO)(bim) moieties of all six cyclotriphosphazene rings were compatible with previously observed bond parameters of cyclotriphosphazene derivatives[54,55] and they can be attributed to electron-releasing character of phenyl groups.

The crystal structure of compound **5** consists of two *cis*-dibenzimidazole substituted phosphazene (**4a**) molecules joined together by Cu_2Cl_2 bridge (Figure 6). The dinuclear structure was centrosymmetric and the asymmetric unit contains only one independent Cu(II) centre and the second one was generated by symmetry operation [symmetry code (#): −x+1, −y, −z]. Each five-coordinated Cu(II) ion was surrounded by two benzimidazole nitrogen atoms as well as one terminal and two bridging chlorides, which formed a distorted square pyramidal geometry [Addison parameter (τ): 0.10].[56] In the square plane, the Cu(II) was coordinated by two N atoms and two chlorides in *trans* arrangement [NNCl(μ-Cl) donor set] and one (μ-Cl) chloride ligand in the axial position. The Cu-N bond were 1.990(4)Å and 2.004(4)Å. The equatorial Cu-Cl bonds [2.3037(14)Å and 2.3102(12)Å] were shorter than the axial one [2.6426(14)Å]. The Cl2 and the centrosymmetric Cl2# ions served to bridge the two Cu(II) centers and the bridging two chloride ligands were bound asymmetrically to both copper atoms (Table 2). Two Cu(II) centers were close to each other with a Cu···Cu distance of 3.5187(9) Å. The Cl2-Cu1-Cl2# and Cu1-Cl2#-Cu1# angles for the 4-membered ring are almost orthogonal [89.71(4)° and 90.29(5)°]. The N–Cu–N arrangement was almost linear with an angle of 174.13(15)° and the two coordinated imidazole rings were arranged in almost coplanar arrangement with respect to the copper atom with only a 6.76° angle between them (Figure S16 in supporting file). All these parameters were compatible with those previously observed for similar bis(μ-chloro)Cu(II) complexes.[51,57-59]

View Article Online
DOI: 10.1039/C7DT01134B

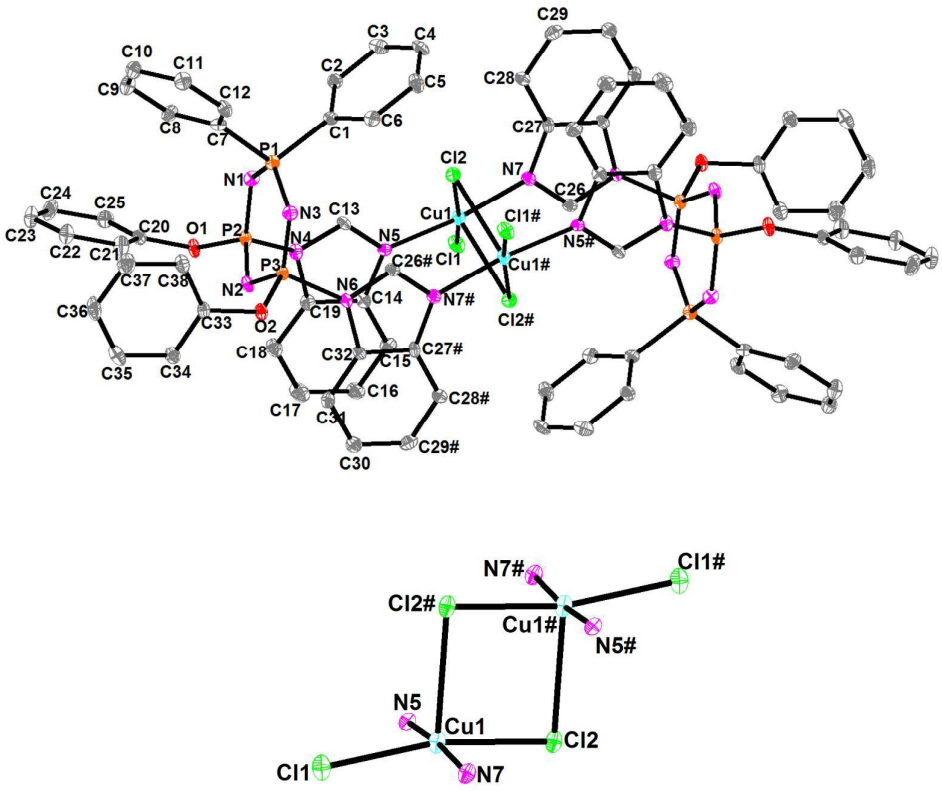

Figure 6. Crystal structures of compound **5** with the atom-numbering scheme. Displacement ellipsoids are drawn at the 30% probability level. The hydrogen atoms have been omitted for clarity. [Symmetry code: (#) −x+1, −y, −z]

A close investigation of the crystal structures of compounds **2a, 3a,b, 4a,b**, and **5** showed that there are weak CH···N and CH···π inter-molecular interactions which were effective in the stabilization of their unit cell (Figures S17-S22 and Tables S1-S6 in supporting file). Especially in the crystal packing of compound **5** the weak π···π intermolecular interactions stabilized tubular channel formation along *a* direction (Figure S22 in supporting file).

Table 1. X-ray crystallographic data and refinement parameters for compounds **2a**, **3a**, **3b**, **4a**, **4b** and **5.**

Compound	**2a**	**3a**	**3b**	**4a**	**4b**	**5**[a]
Empirical formula	$C_{24}H_{20}Cl_2N_3O_2P_3$	$C_{30}H_{26}N_7O_2P_3$	$C_{30}H_{26}N_7O_2P_3$	$C_{38}H_{30}N_7O_2P_3$	$C_{38}H_{30}N_7O_2P_3$	$C_{76}H_{60}Cl_4Cu_2N_{14}O_4P_6$
Formula weight	546.24	609.49	609.49	709.60	709.60	1688.08
Temperature (K)	120(2)	173(2)	173(2)	173(2)	120(2)	173(2)
Crystal system	Monoclinic	Monoclinic	Monoclinic	Monoclinic	Triclinic	Monoclinic
Space group	*P21*	*P21/c*	*P21/n*	*P21/n*	*P-1*	*P21/c*
a (Å)	7.6214(2)	15.243(3)	10.8586(14)	19.144(2)	9.3179(4)	8.6840(5)
b (Å)	17.2180(4)	8.429(2)	16.050(2)	8.3339(10)	11.1854(5)	15.3755(9)
c (Å)	9.4330(2)	23.943(6)	17.562(2)	21.679(2)	16.7744(7)	31.2787(18)
					81.422(2)	
β (°)	92.3800(17)	106.110(16)	106.757(4)°	104.241(8)	89.989(2)	92.348(5)
					79.340(2)	
Volume (Å^3)	1236.78(5)	2955.5(12)	2930.7(7)	3352.5(6)	1698.24(13)	4172.9(4)
Z	2	4	4	4	2	2
Density (calc, Mg/m^3)	1.467	1.370	1.381	1.406	1.388	1.344
Absorption coeff. (mm^{-1})	0.485	0.243	0.245	0.225	0.222	0.807
F(000)	560	1264	1264	1472	736	1724
θ_{max} (°)	28.31°	24.99	26.37	24.99	28.36	25.00
Reflections collected	22613	21325	24599	31786	29301	29425
Independent reflections	6139	5146	5990	5863	8423	7017
R_{int} (merging R value)	0.0481	0.1535	0.0494	0.1560	0.0320	0.1592
Parameters	307	379	379	451	451	478
R ($F^2>2\sigma F^2$)	0.0357	0.0710	0.0411	0.0598	0.0407	0.0667
wR (all data)	0.0732	0.1867	0.1097	0.1676	0.1016	0.1584
Goodness-of-fit on F^2	1.052	1.019	1.034	1.024	1.011	0.980

[a] The unit cell of 5 had a disordered solvent molecule which couldn't be modelled.

View Article Online
DOI: 10.1039/C7DT01134B

Table 2. The selected bond and conformational parameters for compounds **2a**, **3a**, **3b**, **4a**, **4b** and **5**.

	2a	**3a**	**3b**	**4a**	**4b**	**5**
Phosphazene Ring						
	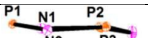	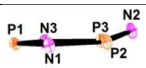	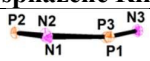	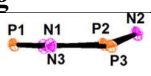		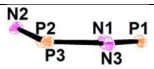
Max. deviation	0.0785(12) (P2)	0.1065(16) (P3)	0.1018(16) (N3)	0.1177(13) (P2)	0.1487(15) (N1)	0.181(4) (N2)
Puckering Amplitude(Q)	0.151(2)	0.196(3)	0.1565(13)	0.223(2)	0.2489(11)	0.260(3)
Theta(°)	168.0(8)	57.8(9)	105.0(5)	62.2(5)	93.6(3)	63.9(7)
Phi(°)	284(4)	191.9(10)	107.6(5)	168.6(7)	232.9(3)	175.4(8)
P1-N1	1.606(3)	1.603(3)	1.6091(16)	1.609(3)	1.6064(14)	1.608(4)
P1-N3	1.610(3)	1.611(4)	1.6122(16)	1.614(3)	1.6144(15)	1.614(4)
P2-N1	1.564(3)	1.563(4)	1.5693(16)	1.567(3)	1.5743(15)	1.565(4)
P2-N2	1.587(3)	1.583(4)	1.5841(16)	1.587(3)	1.5814(15)	1.587(4)
P3-N2	1.584(3)	1.576(3)	1.5841(16)	1.589(3)	1.5879(14)	1.589(4)
P3-N3	1.566(3)	1.559(3)	1.5725(16)	1.565(3)	1.5677(15)	1.561(4)
N1-P1-N3	115.86(14)	115.44(18)	116.40(8)	115.64(15)	115.78(7)	116.2(2)
N1-P2-N2	117.85(15)	119.20(19)	117.50(8)	118.05(16)	118.57(8)	118.2(2)
N2-P3-N3	118.67(14)	118.3(2)	118.58(8)	117.94(16)	119.16(8)	118.0(2)
P1-N1-P2	121.95(15)	122.0(2)	122.80(10)	122.01(18)	121.04(9)	121.3(3)
P2-N2-P3	120.54(18)	118.6(2)	121.92(10)	119.04(18)	119.63(9)	118.1(3)
P1-N3-P3	121.64(17)	122.5(2)	120.74(10)	122.6(2)	120.85(9)	121.8(2)
Substituent moiety						
P-C	1.790(3)	1.792(5)	1.7988(18)	1.796(4)	1.7965(17)	1.781(5)
	1.793(3)	1.789(5)	1.8039(19)	1.790(3)	1.7932(18)	1.797(5)
P-O	1.581(2)	1.580(3)	1.5867(14)	1.585(3)	1.5849(12)	1.574(3)
	1.581(2)	1.581(3)	1.5879(14)	1.589(2)	1.5872(13)	1.575(4)
P-N		1.700(4)	1.7016(16)	1.681(3)	1.6904(15)	1.704(4)
		1.691(4)	1.6975(16)	1.683(3)	1.6869(15)	1.707(4)
P-Cl	2.0153(12)					
	2.0173(12)					
C-P-C	109.11(15)	106.4(2)	107.90(8)	106.60(16)	109.21(8)	107.3(2)
N-P-O		97.59(19)	97.14(8)	99.30(14)	96.94(7)	98.95(18)
		99.25(18)	97.36(7)	96.99(14)	99.65(7)	98.63(19)
Cl-P-O	96.35(10)					
	97.19(9)					

Coordination part of compound 5					
Cu1-N5	1.990(4)	**N5-Cu1-N7**	174.13(15)	**N5-Cu1-Cl1**	90.99(11)
Cu1-N7	2.004(4)	**Cl1-Cu1-Cl2**	168.24(6)	**N5-Cu1-Cl2**	89.40(11)
Cu1-Cl1	2.3037(14)	**Cl1-Cu1-Cl2#**	102.01(5)	**N5-Cu1-Cl2#**	92.74(11)
Cu1-Cl2	2.3102(12)	**Cl2-Cu1-Cl2#**	89.71(4)	**N7-Cu1-Cl1**	88.32(12)
Cu1-Cl2#	2.6426(14)	**Cu1-Cl2#-Cu1#**	90.29(5)	**N7-Cu1-Cl2**	90.10(11)
Cu1-Cu1#	3.5187(9)			**N7-Cu1-Cl2#**	93.11(12)
symmetry code (#) for **5**: −x+1, −y, −z					

View Article Online
DOI: 10.1039/C7DT01134B

2.3. Configurational analysis of compounds 3a,b, 4a,b

Tetra-coordinated, pentavalent phosphorus atoms in hexachlorocyclotriphosphazene, $N_3P_3Cl_6$, are potential chiral centers as in organic compounds having tetrahedral carbon atoms.[48] A non-geminal di-substitution on the $N_3P_3Cl_6$ generates *cis* and *trans* isomers. The *trans* isomer containing two equal chiral centers is chiral and exists as two enantiomers (racemate, *RR/SS*) while the *cis*-isomer containing two equal chiral centers is not chiral (meso, *RS*) because of having a plane of symmetry.[48] Considering the cyclotriphosphazene ring is planar, in terms of centers of chirality its structure was commonly drawn by a stick diagram resulting from projection of the structure perpendicular to the plane of the ring.[48] Therefore, the structures of compounds **3a**,**b**; **4a**,**b** were given by the stick diagram representations that make easy to show the configuration on the each phosphorus as stereogenic center without using wedges and dashes (Figure 7).

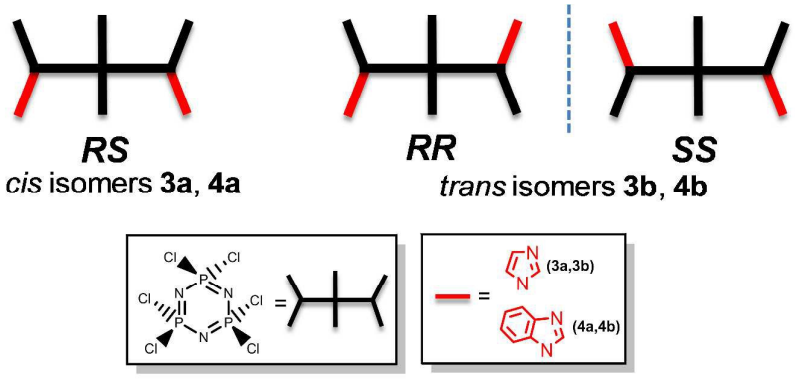

Figure 7. The stick diagram representations of compounds **3a**,**b**; **4a**,**b**.

By analogy with previous work on the stereochemistry of disubstituted *cis* and *trans* isomers of $N_3P_3Cl_6$, in generally the ^{31}P NMR signals on addition of the chiral shift reagent (CSR) or chiral solvating agent (CSA) of *trans* isomer split into two lines of equal intensity corresponding to the separate enantiomers, whereas the NMR signals of *cis* isomer should be unaffected except for changes in chemical shift.[48] In this study, the stereogenic properties of the compounds were supported by ^{31}P NMR spectroscopy on addition of a CSA, (*R*)-(+)-2,2,2-trifluoro-1-(90-anthryl)ethanol. It was found that all ^{31}P NMR signals of compounds **3a**,**b** and **4a**,**b** exhibit chemical shift changes indicating complexation with the CSA. On

View Article Online
DOI: 10.1039/C7DT01134B

addition of a CSA at a 50:1 mol ratio, >P(OPh)(Azoles) peaks of compounds **3b**, **4b** separate into two lines of equal intensity consistent with **3b**, **4b** existing as racemate (*RR/SS*), but CSA does not cause extra splitting of the NMR peaks of compound **3a**, **4a** because they are meso (*RS*) diastereoisomers as expected.[48] As the example, the proton-decoupled ^{31}P NMR spectra of a mixture of compounds **3a**,**b** and after added CSA at a 50:1 mol ratio were given in Figure 8. The changes in ^{31}P NMR chemical shifts and separations of signals of compounds **3a**,**b** and **4a**,**b** at a 50:1 mol ratio of CSA were summarized Table 3.

Structures of **3a**,**b** and **4a**,**b** were also confirmed by X-ray crystallography that compounds **3a**, **4a** are *cis* diastereoisomers and **3b**, **4b** are *trans* diastereoisomers consistent with the CSA addition results.

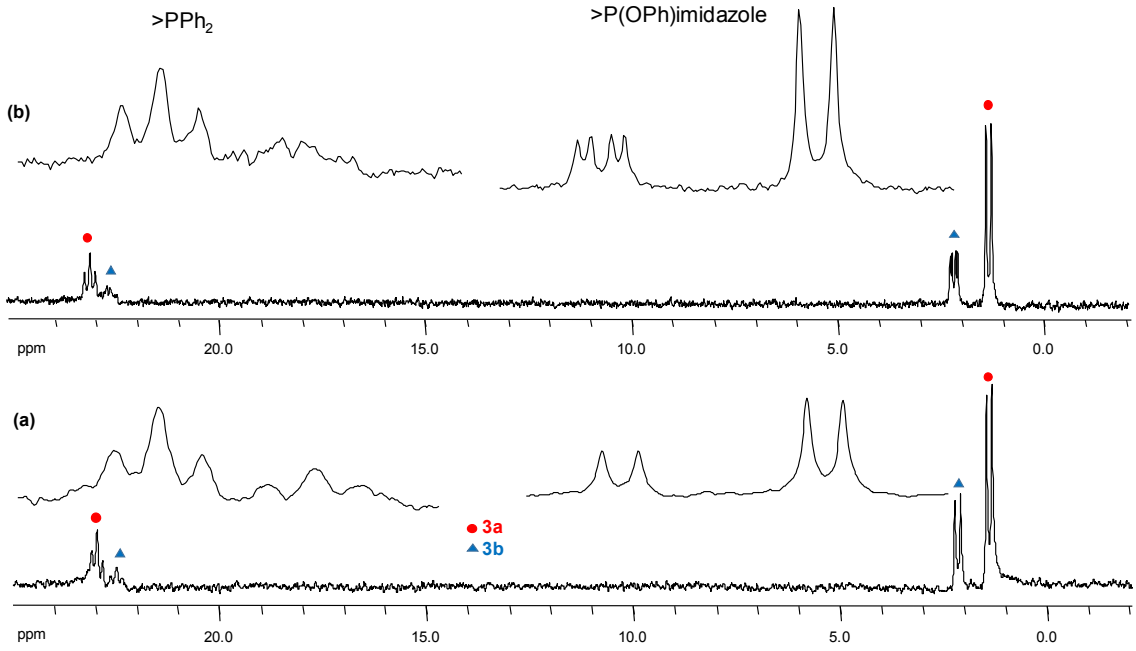

Figure 8. Proton-decoupled ^{31}P NMR spectra of (a) a mixture of **3a**,**b** and expansion of signals of the >PPh_2 and >P(OPh)(imidazole) moieties; (b) a mixture of **3a**,**b** with added CSA at *ca*. 50:1 mole ratio and expansion of signals of the >PPh_2 and >P(OPh)(imidazole) moieties in $CDCl_3$ solution.

View Article Online
DOI: 10.1039/C7DT01134B

Table 3. ^{31}P NMR parameters of compounds **2a**,**b**;**3a**,**b** and **4a**,**b**.[a]

Compound	Chemical shifts / ppm			^{2}J(PP) / Hz
	> *P(OPh)Az*	> *P(OPh)Cl*	>PPh_2	
(a) Assignment of signals				
2a		16.61	22.00	25.80
2b[b]		16.66	22.07	24.70
3a	2.51		23.34	27.40
3b	3.16		22.72	27.50
4a	1.51		22.82	27.00
4b	2.25		22.32	27.30
(b) Change of chemical shift (ppb) on addition of CSA in 50:1 mole ratio				
3a	-184		170	27.20
3b	-43		172	27.20
4a	-115		144	26.70
4b	-18		109	27.20
(c) Separation of signals (ppb) on addition of CSA in 50:1 mole ratio				
3a	[c]		[c]	
3b	30		59	
4a	[c]		[c]	
4b	54		[d]	

[a]202.25 MHz ^{31}P NMR measurements in $CDCl_3$ solutions at 298K analysed as AX_2 spin systems. Chemical shifts referenced to external H_3PO_4; [b] it has been observed in the ^{31}P NMR spectra of reaction mixture; [c] no separation of ^{31}P NMR peaks observed; [d] peaks have not seen clearly because of background noise.

2.4. Spectral studies

The metal detecting behavior of imidazole, **3** (a mixture of **3a** + **3b**), and benzimidazole, **4** (a mixture of **4a** + **4b**), isomers were initially investigated. The UV-Vis and fluorescence spectroscopic experiment of compounds **3** and **4** were measured in acetonitrile: water (1:1) and acetonitrile with dilute solutions of 50 μM and 10 μM, respectively. All of the spectral measurements were carried out in a spectroscopic cuvette by using a micropipette at 25 °C. 50 μM compound **3** and 10 μM compound **4** were prepared from their 0.01 M stock solutions. Compound **3** exhibited absorption bands centered around 260-267 nm, and maximum absorption bands of **4** nm were showed at 272-281 nm. The fluorescence maximums of **3** and **4** were observed at 284 nm and 294 nm, respectively, when excited at 250 nm which attributed to phenol/phenyl and benzimidazole moieties (Figure 9).[60,61] The origin of the fluorescence signals of compounds **3a-b** and **4a-b** originated from π-π* transition of phenol/phenyl and/or benzimidazole moieties as expected.[62,63]

View Article Online
DOI: 10.1039/C7DT01134B

To evaluate the fluorescence probe properties of compounds **3** and **4** in acetonitrile: water (1:1) and acetonitrile, 100 μM different competitive metal ions (Al^{3+}, Li^{+}, Na^{+}, K^{+}, Cs^{+}, Mg^{2+}, Ca^{2+}, Ba^{2+}, Hg^{2+} , Pb^{2+}, Mn^{2+}, Cd^{2+}, Ag^{+}, Ni^{2+}, Cu^{2+}, Zn^{2+}, Co^{2+}, Cr^{3+}, Fe^{2+} and Fe^{3+}) were added to solutions of **3** and **4.** The UV-Vis spectra of **3** and **4** nearly unchanged upon the addition of 100 μM of various metal ions except for Cu^{2+}, Fe^{2+}, Fe^{3+} and Ni^{2+} (Figures 10a,b). In the case of Cu^{2+}, the new absorption bands were observed at 310 nm and 461 nm which can attributed charge transfer between metal and ligands as expected.[64] According to Figure 11a,b, fluorescence signals of **3** and **4** significantly quenched by upon addition of 100 μM Cu^{2+}, Fe^{2+}, Fe^{3+}, Zn^{2+} and Ni^{2+} when other various metal ions cause minor change.

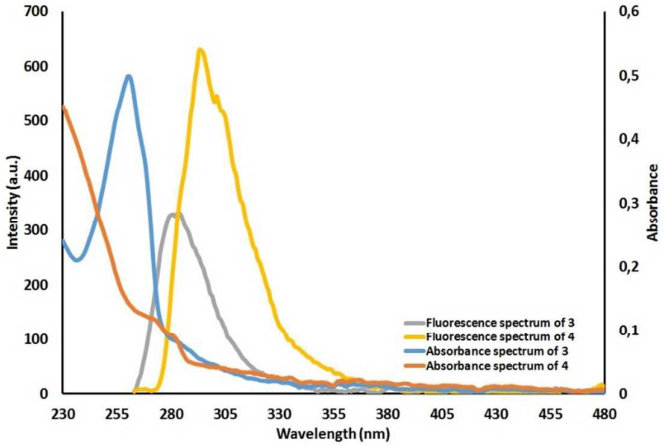

Figure 9. Absorption and fluorescence responses of compound **3** (50 μM) and **4** (10 μM) in ACN: Water (1:1) and ACN, respectively (Excitation wavelength= 250 nm).

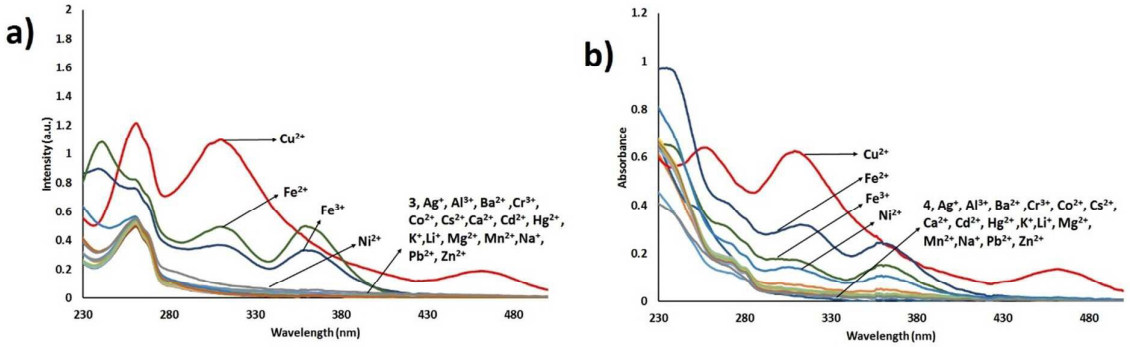

View Article Online
DOI: 10.1039/C7DT01134B

Figure 10. Absorption responses of **a)** compound **3** (50 μM) in ACN: Water (1:1) and **b) 4** (10 μM) in ACN upon the addition of 100 μM various metal.

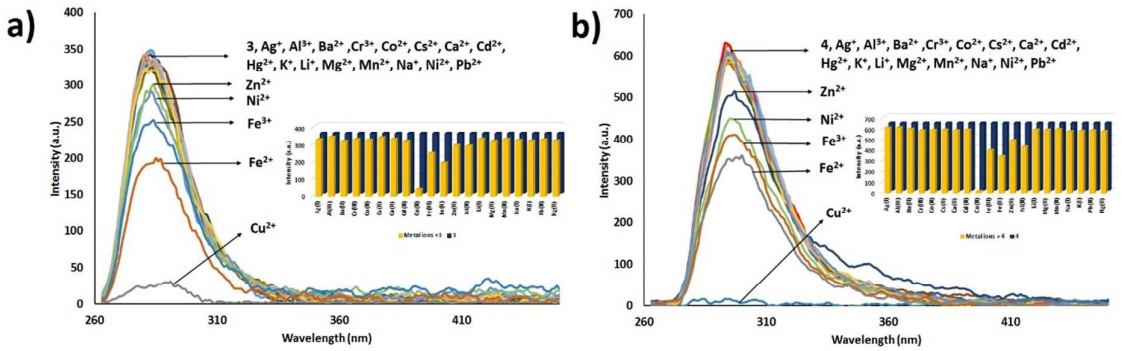

Figure 11. Fluorescence responses of **a)** compound **3** (50 μM) in ACN: Water (1:1) and **b) 4** (10 μM) in ACN upon the addition of 100 μM various metal. **Insets:** Metal ions selectivity of compound **3** (50 μM) in ACN: Water (1:1) and **b) 4** (10 μM) in ACN. The dark blue bars represent the fluorescent intensity of **3** and **4**. The yellow bars represent the fluorescent intensity of **3** and **4** and various ions (Excitation wavelength= 250 nm).

The results of UV-vis and fluorescence signals of imidazole or benzimidazole isomers **(3** or **4)** indicated that these forms cannot be used as a potential specific fluorescent probe for selective detection of any metal ions. After the separated the two configurational isomers (*cis*- or *trans*) of **3** and **4,** optical properties of each individual isomer (**3a, 3b, 4a** or **4b)** were re-investigated by UV-vis absorption and fluorescence spectroscopies. The fluorescence properties of 50 μM **3a, 3b** and 10 μM **4a**, **4b** were studied in various solvents such as water, cyclohexane (CH), dichloromethane, THF, ethanol, acetonitrile, acetonitrile: water (1:1) and acetonitrile (5:1). According to Figure 12a-d, the maximum fluorescence signals of 50 μM **3a** and **3b** were obtained in ACN: Water (1:1) at 284 nm. The fluorescence spectra of 10 μM **4a** and **4b** showed that maximum signal at 294 nm were obtained in ACN. For this reason, ACN: Water (1:1) was chosen as solvent mixture for **3a** and **3b** and ACN for **4a** and **4b** which is also water miscible organic solvent, to use in our study. To investigate concentration effect on optical properties of **3a, 3b, 4a** and **4c** different concentration of these compounds were prepared and 50 μM for **3a** and **3b**, 10 μM of **4a** and **4b** chosen for spectral studies (Figure 13a,b). As shown Figure 13, the absorption and fluorescence maxima of **3a** and **3b, 4a** and **4b** were the identical to their isomer mixtures **3** and **4.** The fluorescence probe properties of **3a, 3b, 4a** and **4b** against competitive metal ions were investigated. For these purpose, 100 μM of

View Article Online
DOI: 10.1039/C7DT01134B

various metal ions (Al^{3+}, Li^{+}, Na^{+}, K^{+}, Cs^{+}, Mg^{2+}, Ca^{2+}, Ba^{2+}, Hg^{2+}, Pb^{2+}, Mn^{2+}, Cd^{2+}, Ag^{+}, Ni^{2+}, Cu^{2+}, Zn^{2+}, Co^{2+}, Cr^{3+}, Fe^{2+} and Fe^{3+}) were added to ACN: Water (1:1) solutions of **3a** and **3b** (10 μM), ACN solutions of **4a** and **4b** (50 μM).

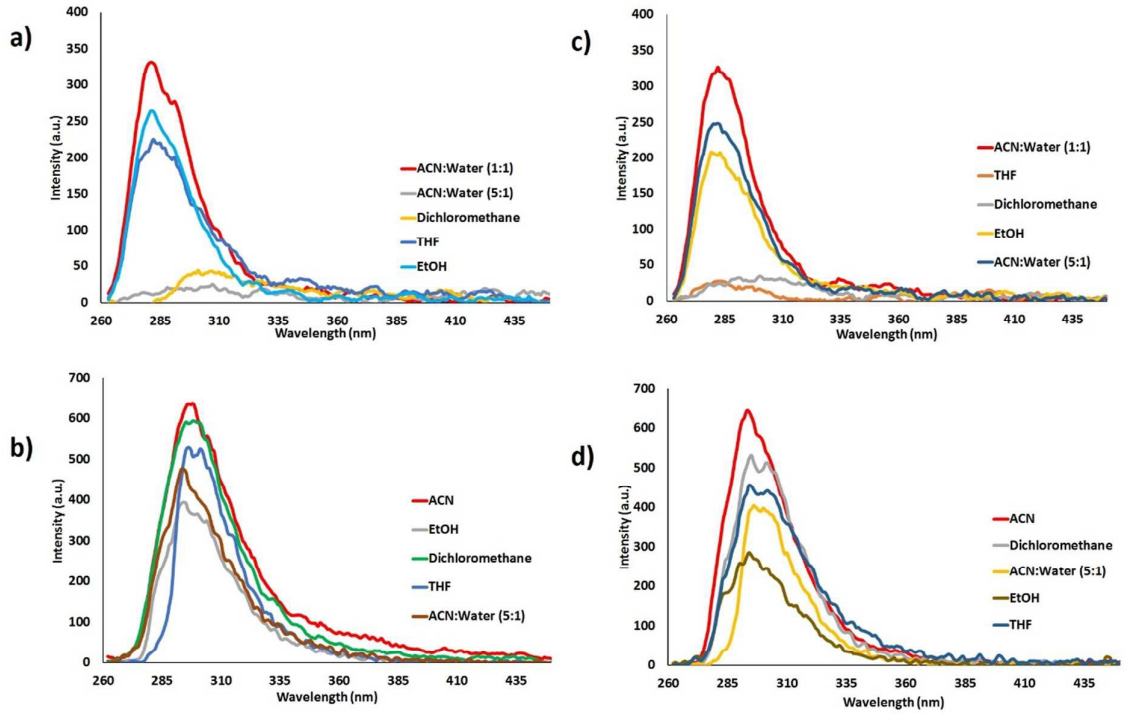

Figure 12. Fluorescence responses of **a)** 50 μM **3a b)** 50 μM **3b c)** 10 μM **4a** and **d)** 10 μM **4b** in different solvent (Excitation wavelength= 250 nm).

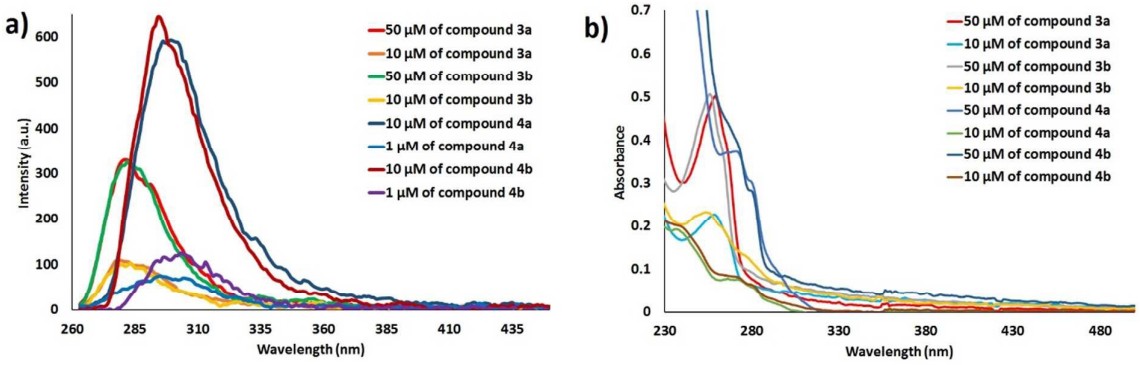

View Article Online
DOI: 10.1039/C7DT01134B

Figure 13. a) Fluorescence responses **b)** UV-VIS absorption responses of **3a, 3b, 4a** and **4b** in ACN: Water (1:1) and ACN solution in different concentrations (Excitation wavelength= 250 nm).

As can be seen Figure 14a-d, the UV-Vis spectra of **3a, 3b, 4a** and **4b** nearly unchanged upon the addition of 100 μM of various metal ions except for Cu^{2+}. According to UV-Vis spectra, only addition of Cu^{2+} changed maximum absorption wavelength and new bands appeared at 310 nm and 461 nm. After addition of 100 μM of Cu^{2+}, maximum fluorescence signals completely quenched for **4a**, **4b** and remarkable quenched for **3a**, **3b**, when other competitive metal ions nearly did not affect signals (Figure 15a-d).

To evaluate the influence of pH with all compounds (**3a**-**4b**), whereas other parameters were kept constant, 0.1 mL of Britton-Robinson buffer systems was used to adjust the pH of the solvents from 6.09 to 9.91 and plotted in presence of 100 μM Cu^{2+}. The relative fluorescence intensity of compounds **3a**-**4b** were relatively unaffected by pH 6.09-8.36 as seen from Figure S23. Influence of time was investigated and plotted from 5 second to 120 second in presence of 100 μM Cu^{2+}. After 5 second, relative fluorescence responses of all compound reached maximum value and then nearly did not change after this time as seen from Figure S24. Therefore, the detection of Cu^{2+} ion measurements have done after 10 seconds for consistent and accurate results.

In order to receive more information about binding mechanism of compounds **3a, 3b, 4a** and **4b** towards Cu^{2+}, fluorescence titration experiments were performed in the 0-100 μM Cu^{2+} (Figure 16a-d). According to fluorescence titration curves of compounds **3a** and **3b** (Figure 16a-b) and **4a** and **4b** (Figure 16c-d), fluorescence maxima at 284 nm for **3a, 3b** and 294 nm for **4a, 4b** were gradually decreased and finally almost completely quenched. The highly efficient quenching of Cu^{2+} proposed that fluorophores showed a specific response to Cu^{2+} due to the chelation-enhanced fluorescence quenching effect which was previously reported in the literature.[65,66] This could be attributed to the significant binding of Cu(II) in the nitrogen coordination pocket of fluorophores and could prefer the efficient energy/electron transfer from paramagnetic Cu(II) to the imidazole units.

View Article Online
DOI: 10.1039/C7DT01134B

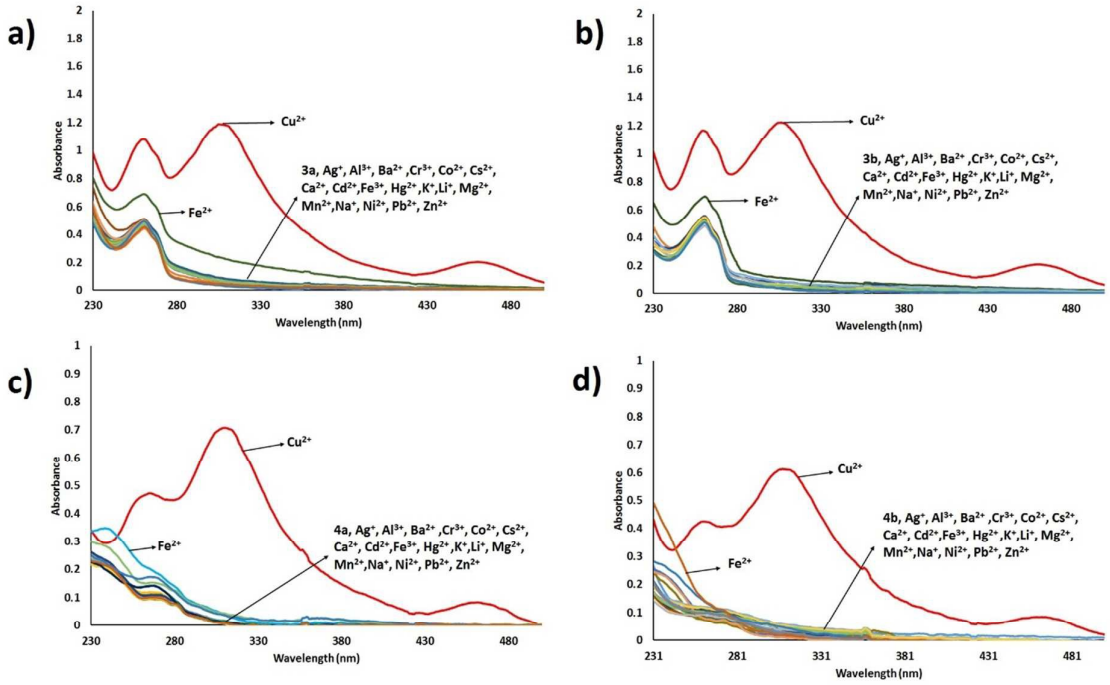

Figure 14. UV-VIS absorption responses of a**) 3a** (50 μM) in ACN: Water (1:1), **b) 3b** (50 μM) in ACN: Water (1:1)**, c) 4a** (10 μM) in ACN and **d) 4b** (10 μM) in ACN upon the addition of 100 μM various metal ions.

View Article Online
DOI: 10.1039/C7DT01134B

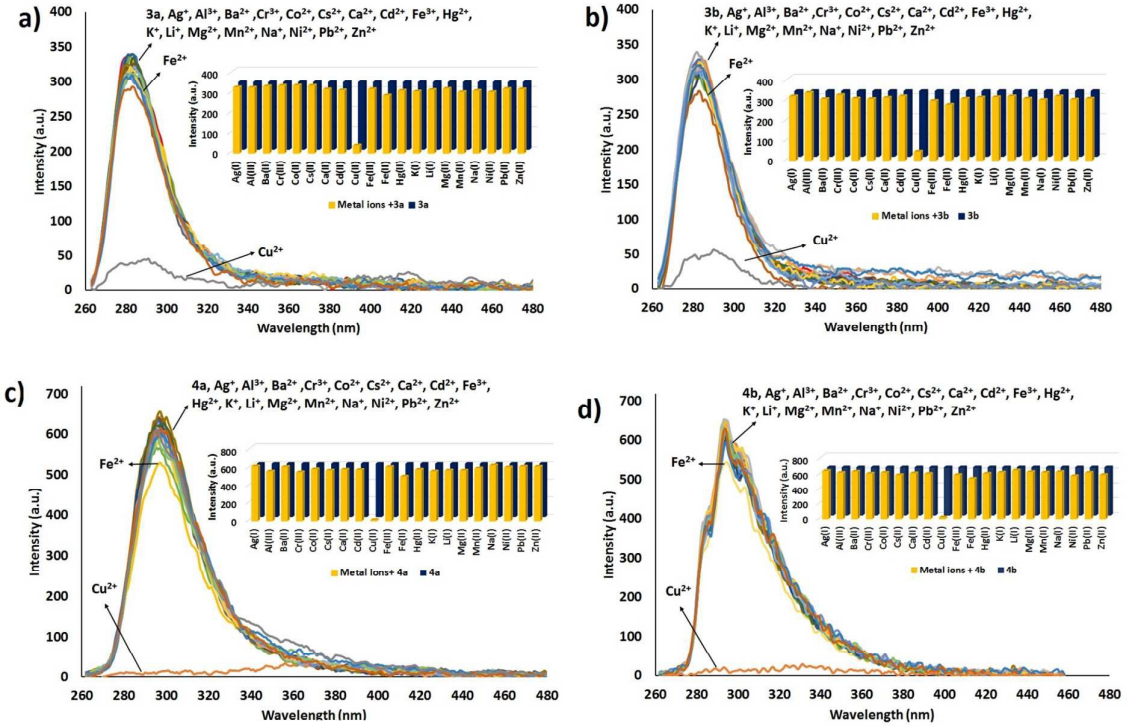

Figure 15. Fluorescence responses of a**) 3a** (50 μM) in ACN: Water (1:1), **b) 3b** (50 μM) in ACN: Water (1:1)**, c) 4a** (10 μM) in ACN and **d) 4b** (10 μM) in ACN upon the addition of 100 μM various metal ions. **Insets:** The dark blue bars represent the fluorescent intensity of compound **3a, 3b, 4a** and **4b**. The yellow bars represent the fluorescent intensity of compound **3a, 3b, 4a** and **4b**-various ions (Excitation wavelength= 250 nm).

The fluorescence titration profiles of **3a**, **3b**, **4a** and **4b** with Cu^{2+} in the range of 0 to 100 μM showed the Cu^{2+} sensitivity of probes. The detection limit of compounds **3a, 3b, 4a** and **4b** for Cu^{2+} ion by fluorescence changes was calculated on the basis of 3σ /K[67-69] and found to be 1.27 μM, 1.54 μM, 1.89 μM and 2.04 μM pointing to the high detection sensitivity (Figure 16 insets). These results suggested that compounds **3a, 3b, 4a** and **4b** can be used for the selective detection of Cu^{2+} in ACN: Water (1:1) and ACN solutions. Precision of the probe is an important analytical parameter for probe application. Therefore, ten measurements were performed for 100 μM of Cu^{2+} under the same conditions for all compounds. The relative standard deviation (% RSD) was calculated as %4.86, %4.41, %4.92 and % 3.74 for compounds **3a, 3b, 4a** and **4b**, respectively. According to these results, high reproducibility can be provided for selected probes.

View Article Online
DOI: 10.1039/C7DT01134B

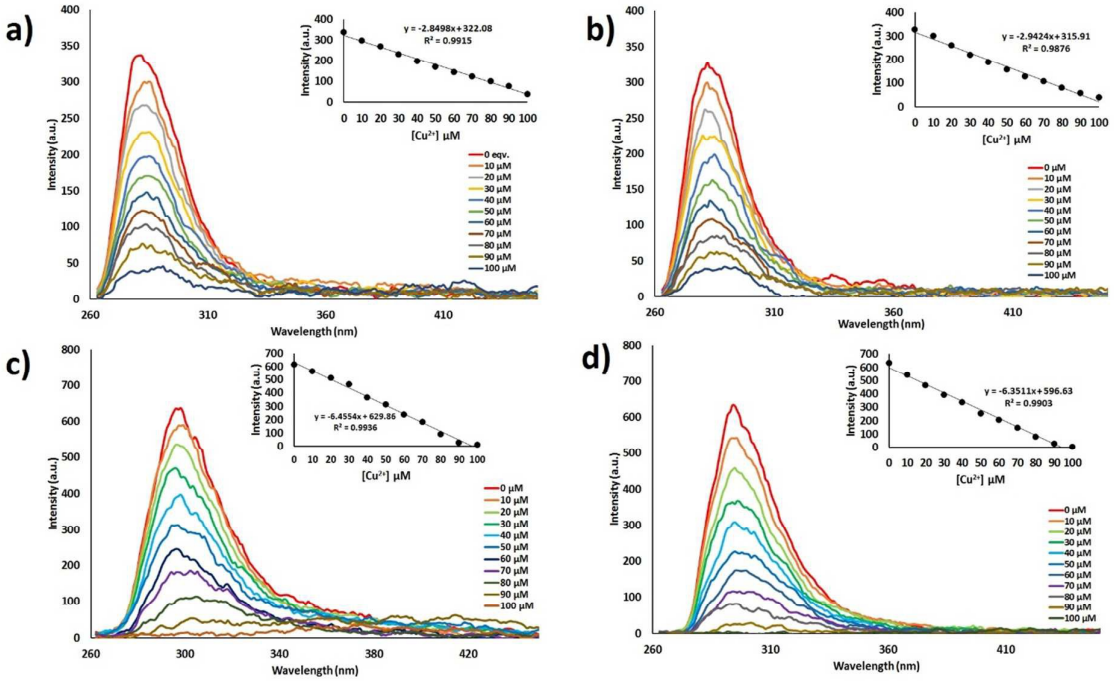

Figure 16. Fluorescence titration of **a) 3a** (50 µM) in ACN: Water (1:1), **b) 3b** (50 µM) in ACN: Water (1:1)**, c) 4a** (10 µM) in ACN and **d) 4b** (10 µM) in ACN with various concentration of Cu^{2+}. (Excitation wavelength= 250 nm). **Inset:** Calibration curve of **3a, 3b, 4a** and **4b** versus Cu^{2+} ions.

A comparison of the UV-Vis spectra of 10 µM compound **4a** + 1 eqv. Cu^{2+} and compound **5** which was complex of 1:1 (mole/mole) compound **4a** and Cu^{2+} was presented at Fig. S29. As shown in Fig. S29, all new absorption bands (310 nm and 461 nm) which can attributed charge transfer between metal and ligand were observed at both 10 µM compound **4a** + 1eqv. Cu^{2+} and compound **5**. According to this result, it can be said that spectroscopic absorption result of 10 µM compound **4a** + 1eqv. Cu^{2+} is consistent with the crystal structure of compound **5**.

2.5. Metal-Ion complex formation of ligands 3a,b and 4a,b

Job's plot analyses were used to investigate the stoichiometry between ligands and Cu^{2+} (Figure 17a-d). The results showed that the maximum fluorescent emission intensity of all ligands and Cu^{2+} complexes appeared at 0.5, which indicated that **3a, 3b, 4a** and **4b**-Cu^{2+} complexes were formed in 1:1 ratio. Furthermore, the association constants, K, of the target complexes were then calculated to be 2.81×10^5 M^{-1}, 2.74×10^5 M^{-1}, 2.46×10^5 M^{-1} and 2.37×10^5

View Article Online
DOI: 10.1039/C7DT01134B

M^{-1} for compounds **3a, 3b, 4a** and **4b**, respectively according to Benesi-Hildebrand equation (a), as shown in Figure 18a-d. In this equation, F is fluorescence signal of compounds after addition of various amount of Cu^{2+} at maximum wavelength, F_0 is fluorescence signal of initial compounds at maximum wavelength and F_{max} is maximum fluorescence signal of compounds at maximum wavelength. Although the stereochemistry of compounds were different, the same binding modes with Cu^{2+} (1:1 for L/M) determined using Job's plot and DFT methods led to similar association constants of the isomers.

$$\frac{1}{F - F_0} = \frac{1}{K_a \, x \, (F_{\max} - F_0) \, x \, [Cu^{2+}]} + \frac{1}{F_{\max} - F_0} \quad \text{(a)}$$

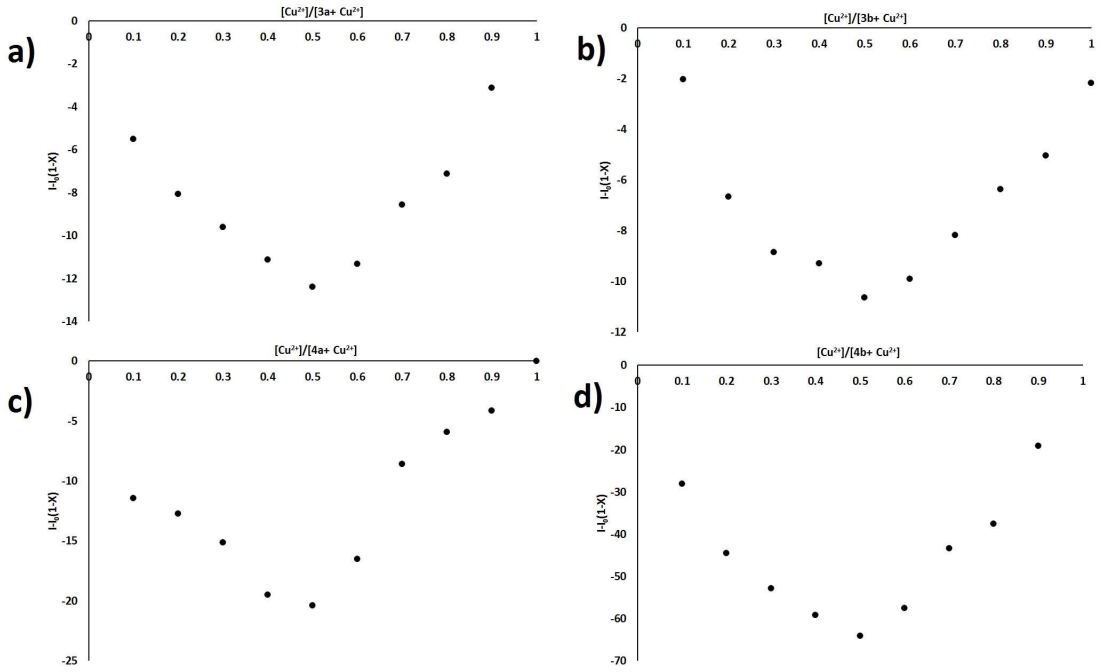

Figure 17. The Job's plot for **a) 3a** (50 μM) and Cu^{2+}, **b) 3b** (50 μM) and Cu^{2+}, **c) 4a** (10 μM) and $Cu^{2+}$and **d) 4b** (10 μM) and Cu^{2+} (Excitation wavelength= 250 nm).

View Article Online
DOI: 10.1039/C7DT01134B

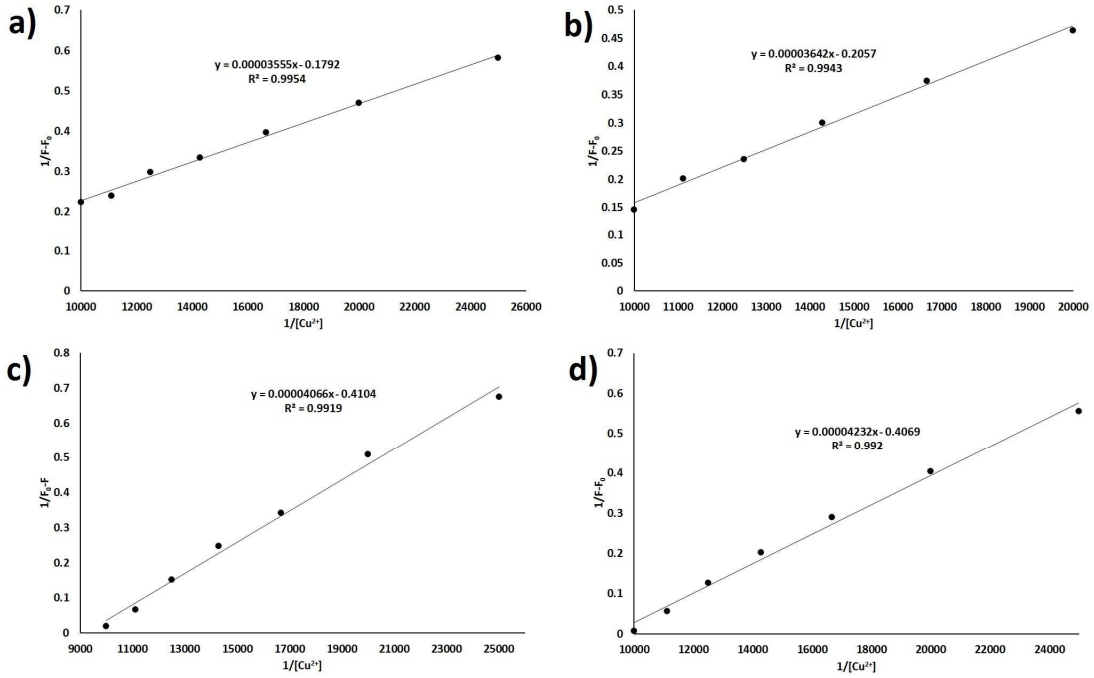

Figure 18. Plot of $1/F\text{-}F_0$ against $1/[Cu^{2+}]$ for **a) 3a** (50 μM) in ACN: Water (1:1), **b) 3b** (50 μM) in ACN: Water (1:1)**, c) 4a** (10 μM) in ACN and **d) 4b** (10 μM) in ACN.

Numerous attempts have been made to prepare Cu^{2+} complexes of all obtained ligands (**3a, 3b, 4a** and **4b**) in order to better understand the coordination of ligands with Cu^{2+} but only binuclear copper complex of compound **4a** was obtained as X-ray suitable pale blue crystal (compound **5**, Figure 6). In the crystal structure, cyclotriphosphazene units of compound **5** linked to "Cu(μ-Cl)2Cu" bridges that the copper(II) ions showed the distorted square-based pyramidal conformation with coordinated through two nongeminal benzimidazole nitrogen atoms. It should be noted that the ring nitrogen atoms of the cyclophosphazene skeleton did not participate in interaction with Cu^{+2}, though many cyclophosphazene ligands having exocyclic groups with two adjacent nitrogen atoms involved in interactions with the ring nitrogen atoms by transition metals.[49-52]

Compound **5**, which is the complex of **4a** with Cu^{+2}, has crystal structure but due to only limited amount of experimental information available for the complexes of **3a**, **3b** and **4b** with Cu^{+2}, the exact coordination complex structures were difficult to identify. Firstly, compound **5** was optimized with DFT m062x and B3LYP/LanL2DZ method and the results was similar to crystal structure analysis. Therefore, this method was studied for the other

View Article Online
DOI: 10.1039/C7DT01134B

compounds **3a**, **3b** and **4b**. Since there is possible structures of square planar, tetrahedral, octahedral and even square based pyramidal structures of transition metal ions with either solvent and/or inorganic anions in the media, Cu^{2+} can complete the first coordination shell with H_2O or Cl^-. Thus, we tried to understand only the qualitative interaction between the metal ion and ligand, instead of identifying the true coordination complex formation. We compared quantum mechanical calculations possible tetrahedral copper complexes formed by Cl^- ions for **3a**, **3b** and **4b**. The optimized structures of the possible the Cu^{2+} complexes were shown in Figure S25-28. The data obtained from DFT calculations were given in Table S7.

The crystal structure of the complex (**5**) has meso configuration with a center of symmetry because of the structural limitation of the *cis*-configured starting material (**4a**) and a similar complexation mechanism can be proposed for *cis*-configured **3a** as shown in the stick diagram in Figure 19a.

As shown in the stick diagram in Figure 19b, a cyclolinear polymer with coppers bridges could be proposed for the complex formation of the *trans*-configured starting materials (**3b** and **4b**) considering with the *trans* structures of ligands and 1:1 (L/M) binding stoichiometry from Job's plot analysis.

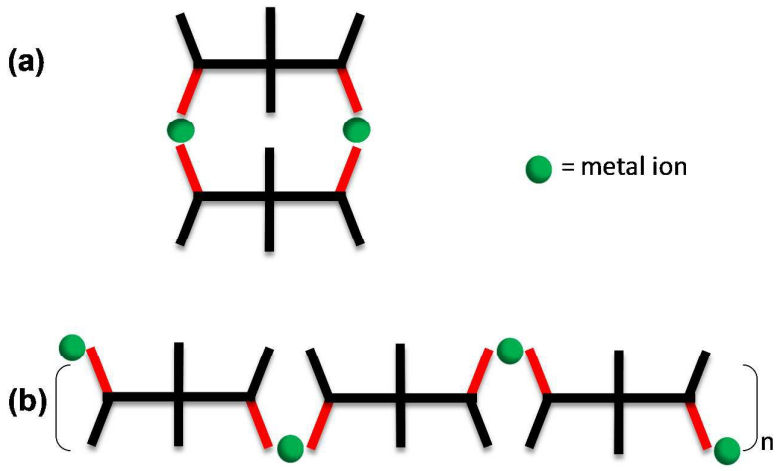

Figure 19. The proposed stick diagram representations of complex formations of *cis* and *trans* geometrical isomers with $CuCl_2$.

View Article Online
DOI: 10.1039/C7DT01134B

3. Experimental

3.1. Materials

The chemicals were obtained commercially and used as received; aluminum chloride (98%), phenol (99%), benzimidazole (99%), *n*-hexane (99%), dichloromethane (99.0%), triethylamine (99%), cyclohexane (99%), ethanol (99%), acetonitrile (99%), deuterated chloroform (for NMR spectroscopy) from Merck, imidazole (99%) from Alfa Aesar, benzene (>98%) and tetrahydrofuran (>99%) from Aldrich. Chiral solvating agent, (*R*)-(+)-2,2,2-trifluoro-1-(9-anthryl)ethanol (CSA) from Sigma. Tetrahydrofuran, THF (Aldrich) was distilled over sodium/potassium alloy under an atmosphere of dry argon. Prior to use the oil in a sodium hydride, 60% dispersion in mineral oil (Merck) was removed by washing with dry *n*-hexane followed by decantation. All reactions were performed under a dry argon atmosphere. Hexachlorocyclotriphosphazene which was purified by crystallisation from *n*-hexane was obtained from Aldrich. Thin layer chromatography (TLC) and column chromatography were carried out on Merck silica gel plates (Kieselgel 60, F254 indicator, 0.25 mm) and silica gel (Kieselgel 60, 70–230 mesh) respectively.

3.2. Equipment

Bruker Daltonics Microflex LT MALDI-TOF mass spectrometers were used to obtain mass spectra. NMR (^{31}P, ^{1}H) spectra were recorded on a Varian INOVA 500 MHz spectrometer in $CDCl_3$ solutions using 85% H_3PO_4 as external reference for ^{31}P and TMS as internal reference for ^{1}H. Electronic absorption spectra were recorded with a Shimadzu 2101 UV spectrophotometer in the UV-visible region. Fluorescence excitation and emission spectra were recorded on a Varian Eclipse spectrofluorometer using 1 cm pathlength cuvettes at room temperature and slit withs were all set to 5 nm.

3.3. X-ray crystallography

Intensity data were recorded on a Bruker APEX II QUAZAR diffractometer. Absorption correction by multi-scan has been applied[70] and space groups were determined using XPREP implemented in APEX2.[71] Structures were determined using the direct methods procedure in SHELXS-97 and refined by full-matrix least squares on F^2 using SHELXL-97.[72] All non-hydrogen atoms were refined with anisotropic displacement factors and C-H hydrogen atoms were placed in calculated positions and allowed to ride on the parent atom. Furthermore, the unit cell of 5 had a disordered solvent molecule which couldn't be modelled. Therefore, the

View Article Online
DOI: 10.1039/C7DT01134B

SQUEEZE command of PLATON[73] was used for removing solvent molecule then the rest of the molecule was refined without solvent. There were two cavities with 381 Å^3 volume and 96 void electron count. The final geometrical calculations and the molecular drawings were carried out with PLATON,[73] MERCURY,[74] and DIAMOND (Version 3.1)[75] programs. Structure determinations have been deposited with the Cambridge Crystallographic Data Centre with references CCDC 1525898-152903 for structures **2a**, **5**, **4b**, **3b**, **4a** and **3a**, respectively.

3.4. DFT Calculations

The full geometry optimization on the basis of crystal structures of compounds **3a**, **3b**, **4b** and **5** were carried out with the density functional theory method by a hybrid functional B3LYP functional (Becke's Three Parameter Hybrid Functional Using the LYP Correlation Functional)[76,77] and Los Alamos National Laboratory 2-Double-Zeta (LanL2DZ) basis set[78] have been chosen in the DFT calculations, in this study. LanL2DZ basis set was used in the calculations in order to make a comparison with the structural parameters of Cu(II) complexes of molecules. Molecular geometry was restricted and all the calculations for compounds are performed using Gaussian 09[79] program package on a TUBITAK ULAKBIM, High Performance and Grid Computing Center (TR-Grid e-infrastructure).

3.5. Synthesis

2,2,4,4-Tetrachloro-6,6-diphenylcyclotriphosphazene $[N_3P_3Cl_4(Ph)_2]$ (**1**)**,** was prepared as described in the literature.[50]

3.5.1. *cis*-$[N_3P_3Cl_2(Ph)_2(OC_6H_5)_2]$ (**2a**) and *trans*-$[N_3P_3Cl_2(Ph)_2(OC_6H_5)_2]$ (**2b**)

To a stirred solution of 2,2,4,4-tetrachloro-6,6-diphenylcyclotriphosphazene $[N_3P_3Cl_4(Ph)_2]$ (**1**) (2.0 g, 4.64 mmol) in 50 mL tetrahydrofuran (THF) was added NaH (0.4 g, 9.28 mmol) under an argon atmosphere. The solution was cooled to 0°C using an ice-bath, phenol (0.88 g, 9.28 mmol) in 20 mL THF was then added dropwise to the stirred mixture under an argon atmosphere. The mixture was stirred for 24 h at room temperature, then precipitate was filtered off and the solvent was removed under reduced pressure. From the crude mixture, a small quantity of compound **2a** and the mostly isomer mixture (**2a** and **2b**) were obtained by column chromatography using dichloromethane/*n*-hexane (1:1) as the mobile phase. **2a** and

View Article Online
DOI: 10.1039/C7DT01134B

2b, 1.2 g, 47%. Compound **2a** was crystallized from dichloromethane/*n*-hexane (1:1), **2a**, 0.07 g, 3%, mp 125°C, M:545.74m/z (calc.545.01), ^{1}H NMR, $CDCl_3$, 298 K, δ (ppm); 7.21-7.87 (m, Ar-*H*), ^{31}P NMR, $CDCl_3$, 298 K, δ (ppm); 16.61 (d, *P*(OPh)Cl), 22.00 (t, *P*Ph_2), ^{2}J(PP)= 25.80 Hz. *Calc*. for $C_{24}H_{20}Cl_2N_3O_2P_3$ requires: C, 52.77; H, 3.69; N, 7.69%; found: C, 52.48; H, 3.53; N, 7.57%

3.5.2. *cis*-$[N_3P_3Cl_2(Ph)_2(OC_6H_5)_2(C_3H_3N_2)_2]$ (**3a**) and *trans*-$[N_3P_3Cl_2(Ph)_2(OC_6H_5)_2(C_3H_3N_2)_2]$ (**3b**)

A mixture of compounds **2a** and **2b** (0.50 g, 0.92 mmol) was dissolved in THF (35 ml) and triethylamine (0.25 ml, 1.84 mmol) was added under an argon atmosphere. Imidazole (0.12 g, 1.84 mmol) dissolved in 15 mL THF was then added dropwise to the stirred solution of mixture of compounds **2a** and **2b** under an argon atmosphere. The mixture was refluxed until TLC indicated complete consumption of the starting compounds **2a** and **2b**. After refluxing for 72h, the mixture was cooled to ambient temperature, then the triethylamine hydrochloride salt formed was filtered off and the solvent was removed under reduced pressure. From the crude mixture, compounds **3a** and **3b** were isolated by column chromatography using tetrahydrofuran/*n*-hexane (2:1) as the mobile phase. Compounds **3a** and **3b** were crystallized from dichloromethane/*n*-hexane (2:1); **3a**, 0.25 g, 45%, mp 130°C, M:609.84m/z (calc.609.51); ^{1}H NMR, $CDCl_3$, 298 K, δ (ppm); 6.91-7.84 (m, Ar-*H*), ^{31}P NMR, $CDCl_3$, 298 K, δ (ppm); 2.51 (d, *P*(OPh)Az), 23.34 (t, *P*Ph_2), ^{2}J(PP)= 27.40 Hz; *Calc*. for $C_{30}H_{26}N_7O_2P_3$ requires: C, 59.12; H, 4.30; N, 16.09%; found: C, 58.63; H, 4.28; N, 15.88%; **3b**, 0.18 g, 32%, mp 150°C, M:609.14m/z (calc.609.51), ^{1}H NMR, $CDCl_3$, 298 K, δ (ppm); 6.89-7.69 (m, Ar-*H*), ^{31}P NMR, $CDCl_3$, 298 K, δ (ppm); 3.16 (d, *P*(OPh)Az), 22.72 (t, *P*Ph_2), ^{2}J(PP)=27.50 Hz. *Calc*. for $C_{30}H_{26}N_7O_2P_3$ requires: C, 59.12; H, 4.30; N, 16.09%; found: C, 58.77; H, 4.17; N, 15.74%;

3.5.3. *cis*-$[N_3P_3Cl_2(Ph)_2(OC_6H_5)_2(C_7H_5N_2)_2]$ (**4a**) and *trans*-$[N_3P_3Cl_2(Ph)_2(OC_6H_5)_2(C_7H_5N_2)_2]$ (**4b**)

A mixture of compounds **2a** and **2b** (0.5 g, 0.92 mmol) was dissolved in THF (35 ml) and triethylamine (0.25 ml, 1.84 mmol) was added under an argon atmosphere. Benzimidazole (0.22 g, 1.84 mmol) dissolved in 15 mL THF was then added dropwise to the stirred solution of mixture of compounds **2a** and **2b** under an argon atmosphere. The mixture was refluxed until TLC indicated complete consumption of the starting compounds **2a** and **2b**. After

View Article Online
DOI: 10.1039/C7DT01134B

refluxing for 72h, the mixture was cooled to ambient temperature, then the triethylamine hydrochloride salt formed was filtered off and the solvent was removed under reduced pressure. From the crude mixture, compounds **4a** and **4b** were isolated as pure by column chromatography using dichloromethane/tetrahydrofuran (20:1) as the mobile phase. Compounds **4a** and **4b** were crystallized from dichloromethane/*n*-hexane (1:1); **4a**, 0.23 g, 36%, mp 158°C, M:710.07m/z (calc.709.63), ^{1}H NMR, $CDCl_3$, 298 K, δ (ppm); 6.93-8.01(m, Ar-*H*), ^{31}P NMR, $CDCl_3$, 298 K, δ (ppm); 1.51 (d, *P*(OPh)Az), 22.82 (t, *P*Ph$_2$), ^{2}J(PP)=27.00 Hz; *Calc*. for $C_{38}H_{30}N_7O_2P_3$ requires: C, 64.32; H, 4.26; N, 13.82%; found: C, 63.55; H, 4.38; N, 13.31%; **4b**, 0.31 g, 48%, mp 178°C, M:710.13m/z (calc.709.63), ^{1}H NMR, $CDCl_3$, 298 K, δ (ppm); 6.81-8.01(m, Ar-*H*), ^{31}P NMR, $CDCl_3$, 298 K, δ (ppm); 2.25 (d, *P*(OPh)Az), 22.32 (t, *P*Ph$_2$), ^{2}J(PP)=27.30 Hz. *Calc*. for $C_{38}H_{30}N_7O_2P_3$ requires: C, 64.32; H, 4.26; N, 13.82%; found: C, 64.18; H, 4.13; N, 13.74%;

3.5.4. Synthesis of compound **5**

Compound **4a** (10 mg, 0.014 mmol) was dissolved in 1 ml dichloromethane in NMR tube and then to this solution, $CuCl_2$ (1.89 mg, 0.014 mmol) dissolved in 1 ml ethanol was added slowly and blue crystals were obtained by slow diffusion; **5**, 1.8 mg (yield 8%), mp>250°C. *Calc*. for $C_{76}H_{60}Cl_4Cu_2N_{14}O_4P_6$ requires: C, 54.07; H, 3.58; N, 11.62%; found: C, 53.98; H, 3.52; N, 11.57%.

4. Conclusion

To summarize, we presented the design, synthesis and configurational analysis of imidazole- or benzimidazole-modified *cis*- and *trans*-cyclotriphosphazenes for the investigation of their detecting properties towards metal ions. Stereochemistry of configurational isomers were determined by X-ray crystallography and ^{31}P NMR spectroscopy on addition of CSA. The results of UV–vis and fluorescence studies demonstrated that the investigated *cis* and *trans* derivatives of cyclotriphosphazene were capable of the selective binding of the Cu^{2+} ions in the presence of other metals (Ag^{+}, Al^{3+}, Ba^{2+}, Cr^{3+}, Co^{2+}, Cs^{2+}, Ca^{2+}, Cd^{2+}, Fe^{2+}, Fe^{3+}, Hg^{2+}, K^{+}, Li^{+}, Mg^{2+}, Mn^{2+}, Na^{+}, Ni^{2+}, Pb^{2+}, Zn^{2+}). Importantly, it was found that the separation of configurational isomers is effective in both selectivity of metal ions and complex formation, particularly for Cu^{2+}. The method of Job's plot indicated the formation of 1:1 complexes between each *cis* and *trans* configurational isomers with copper(II) ions and the proposed structural models were totally different as the dimeric complexes with bis-copper bridges for

View Article Online
DOI: 10.1039/C7DT01134B

cis isomers and cyclolinear polymers via coppers bridges for *trans* isomers. The crystal structure of *cis*-probe-Cu^{2+} determined by single-crystal X-ray crystallographic analysis which also confirmed that the ligands can bind with Cu^{2+} ions in 1:1 ratio. Further studies for their applications in living cell images and diverse structure modification to improve water solubility are in progress.

Supporting Information

Structure determinations have been deposited with the Cambridge Crystallographic Data Centre with references CCDC 1525898-152903 for structures **2a**, **5**, **4b**, **3b**, **4a** and **3a**, respectively. These data can be obtained the supplementary file for this paper and free of charge from The Cambridge Crystallographic Data Centre *via* www.ccdc.cam.ac.uk/data_request/cif . The mass, ^{31}P and ^{1}H NMR spectra data of all the compounds were given in supporting information.

Acknowledgements

We wish to thank TUBITAK ULAKBIM, High Performance and Grid Computing Center (TR-Grid e-Infrastructure) for the calculations reported in the theoretical part of this paper. We also thank to Uğur BOZKAYA for using Gaussian 09 program package.

References

(1) Quang, D. T.; Kim, J. S. Fluoro- and Chromogenic Chemodosimeters for Heavy Metal Ion Detection in Solution and Biospecimens. *Chem. Rev*. **2010**, *110*, 6280–6301.

(2) Que, E. L.; Domaille, D. W. Chang, C. J. Metals in Neurobiology: Probing Their Chemistry and Biology with Molecular Imaging. *Chem. Rev*. **2008**, *108*, 1517–1549.

(3) Barceloux, D. G.; Barceloux, D. *Copper, Clin. Toxicol*. **1999**, *37*, 217–230.

(4) Valentine, J. S.; Doucette, P.A.; Potter, S. Z. Copper-Zinc Superoxidedismutase and Amyotrophic Lateral Sclerosis. *Annu. Rev. Biochem*. **2005**, *74*, 563–593.

(5) Millhauser, G. L.; Copper and The Prion Protein: Methods, Structures, Function, and Disease. *Annu. Rev. Phys. Chem*. **2007**, *58*, 299–320.

(6) Tian, M. Z.; Hu, M. M.; Fan, J. L.; Peng, X. J.; Wang, J. Y.; Sun, S. G., Zhang, R. Rhodamine-Based 'Turn-On' Fluorescent Probe for Cu(II) and Its Fluorescenceimaging in Living Cells. *Bioorg. Med. Chem. Lett*. **2013**, *23*, 2916–2919.

View Article Online
DOI: 10.1039/C7DT01134B

(7) Ma, X.; Tan, Z.; Wei, G.; Wei, D.; Du, Y. Solvent Controlled Sugar–Rhodamine Fluorescence Sensor for Cu^{2+} Detection. *Analyst*, **2012**, *137*, 1436–1439.

(8) Wang; J.; Ruiyi, L.; Xiaohuan, L.; Zaijun, L. Synthesis Of Imidazole-Functionalized Silicon Quantum Dots as"Off-On" Fluorescence Probe For Highly Selective and Sensitive Detection of L-Histidine. *Sensors and Actuators B.* **2016**, *237*, 740–748.

(9) Wang, X.; Xu, T.; Duan, H. Schiff Base Fluorescence Probes for Cu2+Based on Imidazole Andbenzimidazole. *Sensors and Actuators B*. **2015**, *214*, 138–143.

(10) Xu, G.; Wang, J.; Si, G.; Wang, M.; Xue, X.; Wu, B.; Zhou, S. A Novel Highly Selective Chemosensor Based on Curcumin Fordetection of Cu^{2+} and Its Application for Bioimaging. *Sensors and Actuators B*. **2016**, *23*, 0684–689.

(11) Pandey, A. D.; Raghuvir R. Pissurlenkar, S.; Karnik, A. V. New Family of Fluorogenic Azacrown Probes with Identical Cavity Size but Different Electronic Environment Outside the Macrocycle: Effects on Sensitivity of Cu^{2+} Detection. *J. Incl. Phenom. Macrocyc. Chem*. **2015**, *81*, 251–261.

(12) Anbu, S.; Shanmugaraju, S.; Ravishankaran, R.; Karande, A. A.; Mukherjee, P. S. Naphthylhydrazone Based Selective and Sensitive Chemosensors for Cu^{2+} and Their Application in Bioimaging. *Dalton Trans*. **2012**, *41*, 13330–13337.

(13) Ding, Y.; Tang, Y.; Zhu, W.; Xie, Y. Fluorescent and Colorimetric Ion Probes Based on Conjugated Oligopyrroles. *Chem. Soc. Rev*. **2015**, *44*, 1101–1112.

(14) Qian, X.; Xu, Z. Fluorescence Imaging of Metal Ions Implicated in Diseases. *Chem. Soc. Rev*. **2015**, *44*, 4487-4493.

(15) She, M.; Yang, Z.; Hao, L.; Wang, Z.; Luo, T.; Obst, M.; Liu, P.; Shen, Y.; Zhang, S.; Li, J. A Novel Approach to Study The Structure-Property Relationships and Applications in Living Systems of Modular Cu(2+) Fluorescent Probes. *Sci. Rep*. **2016**, *6*, 28972–28979.

(16) Ambrosi, G.; Formica, M.; Fusi, V.; Giorgi, L.; Macedi, E.; Micheloni, M.; Paoli, P.; Rossi, P. A Biphenol-Based Chemosensor for Zn^{II} and Cd^{II} Metal Ions: Synthesis, Potentiometric Studies, and Crystal Structures. *Inorg. Chem*. **2016**, *55*, 7676−7687.

(17) Cotruvo, J. A. Jr.; Aron, T. A.; Ramos-Torresa, K. M.; Chang, C. J. Synthetic Fluorescent Probes for Studying Copper in Biological Systems. *Chem. Soc. Rev*. **2015**, *44*, 4400—4414.

(18) Koneswaran, M.; Narayanaswamy, R. L-Cysteine-Capped ZnS Quantum Dots Based Fluorescence Sensor for Cu^{2+} Ion. *Sensors and Actuators B*. **2009**, *139*, 104–109.

View Article Online
DOI: 10.1039/C7DT01134B

(19) Kim, K. B.; Kim, H.; Song, E. J. Kim, S. Insup Noh and Cheal Kim, A Cap-Type Schiff Base Acting As A Fluorescence Sensor For Zinc(II) And A Colorimetric Sensor For Iron(II), Copper(II), And Zinc(II) In Aqueous Media. *Dalton Trans*. **2013**, *42*, 16569–16577.

(20) Boonmee, C.; Noipa, T.; Tuntulani, T.; Ngeontae, W. Cysteamine Capped Cds Quantum Dots as A Fluorescence Sensor for The Determination of Copper Ion Exploiting Fluorescence Enhancement and Long-Wave Spectral Shifts. *Spectrochim. Acta Part A: Mol. Biomol. Spec.* **2016**, *169*, 161–168.

(21) Sahoo, S. K.; Sharma, D.; Moirangthem, A.; Kuba, A.; Thomas, R.; Kumar, R.; Kuwar, A.; Choi, H.-J.; Basu, A. Pyridoxal Derived Chemosensor for Chromogenic Sensing of Cu^{2+} and Fluorogenic Sensing of Fe^{3+} in Semi-Aqueous Medium. *J. Lumin*. **2016**, *172*, 297–303.

(22) Mariappan, K.; Alaparthi, M.; Caple, G.; Balasubramanian, V.; Hoffman, M. M.; Hudspeth, M.; Sykes, A. G. Selective Fluorescence Sensing of Copper(II) and Water via Competing Imine Hydrolysis and Alcohol Oxidation Pathways Sensitive to Water Content in Aqueous Acetonitrile Mixtures. *Inorg. Chem*. **2014**, *53*, 2953−2962.

(23) Wang, M.; Yan, F.; Zou, Y.; Chen, L.; Yang, N.; Zhou, X. Recognition of Cu^{2+} and Hg^{2+} in Physiological Conditions by a New Rhodamine Based Dual Channel Fuorescent Probe. *Sensors and Actuators B* **2014**, *192*, 512–521.

(24) Chen, J.; Li, Y.; Lv, K.; Zhong, W.; Wang, H.; Wu, Z.; Yi, P.; Jiang, J. Cyclam-Functionalized Carbon Dots Sensor for Sensitive and Selective Detection of Copper(II) Ion and Sulfide Anion in Aqueous Media and its Imaging in Live Cells. *Sensors Actuators B* **2016**, 224, 298–306.

(25) Guo, Y.; Yang, L.; Li, W.; Wang, X.; Shang, Y.; Li, B. Carbon Dots Doped with Nitrogen and Sulfur and Loaded with Copper(II) as a "Turn-On" Fluorescent Probe for Cystein, Glutathione and Homocysteine. *Microchimica Acta* **2016**, *183*, 1409–1416.

(26) Wang, M.; Wang, J. G.; Xue, W. J.; Wu, A. X. A Benzimidazole-Based Ratiometricfluorescent Sensor for Cr^{3+} and Fe^{3+} in Aqueous Solution. *Dyes Pigments*. **2013**, *97*, 475–480.

(27) Junga, H. J.; Singha, N.; Jang, D. O. Highly Fe^{3+} Selective Ratiometric Fluorescent Probe Based on Imine-Linked Benzimidazole. *Tetrahedron Lett*. **2008**, *49*, 2960–2964.

(28) Zhao, M.; Deng, Z.; Tang, J.; Zhou, X.; Chen, Z.; Li, X.; Yanga, L.; Ma, L.-J. 2-(1-Pyrenyl) Benzimidazole as a Ratiometric and "Turn-On" Fluorescent Probe for Iron(III) Ions in Aqueous Solution. *Analyst*, **2016**, *141*, 2308–2312.

View Article Online
DOI: 10.1039/C7DT01134B

(29) Bian, N.; Chen, Q.; Qiu, X.-L.; Qi, A.-D.; Han, B.-H. Imidazole-Bearing Tetraphenylethylene: Fluorescent Probe for Metal Ions Based on AIE Feature. *New J. Chem.*, **2011**, *35*, 1667–1671.

(30) Jeyanthi, D.; Iniya, M.; Krishnaveni, K.; Chellappa, D. A Ratiometric Fluorescent Sensor for Selective Recognition of Al^{3+} Ions Based On A Simple Benzimidazole Platform. *RSC Adv.*, **2013**, *3*, 20984–20989.

(31) Liua, J.; Menga, X.; Duana, H. Xub, T.; Dinga, Z.; Liuc, Y.; Lucia, L. Two Schiff-Base Fluorescence Probes Based on Triazole Andbenzotriazole for Selective Detection of Zn^{2+}. *Sensors Actuators B*. **2016**, *227*, 296–303.

(32) Zhong, K.; Cai, M.; Hou, M. S.; Bian, Y.; Tang, L. A Simple Benzimidazole Based Fluorescent Sensor for Ratiometric Recognition of Zn^{2+} in Water. *Bull. Korean Chem. Soc*. **2014**, *35*, 489–493.

(33) Zhao, B.; Fang, Y.; Ma1, M.; Deng, Q. G.; Xu, Y.; Wang, L. A New On-Fluorescent Sensor for Ag^{+} Based on Benzimidazole Bearing Bis(Ethoxycarbonylmethyl)Amino Groups. *Heterocyc. Commun*. **2015**, *21*, 211–214.

(34) Tanga, L.; Caia, M.; Huanga, Z.; Zhonga, K.; Houa, S.; Biana, Y.; Nandhakumar, R. Rapid and Highly Selective Relay Recognition of Cu(II) and Sulfide Ions by a Simple Benzimidazole-Based Fluorescent Sensor in Water. *Sensors Actuators B*, **2013**, *185*, 188–194.

(35) Yea, H.; Gea, F.; Zhoub, M. Y.; Liua, J. T.; Zhaoa, B. X. A New Schiff Base Fluorescent Probe for Imaging Cu^{2+} In Living Cells. *Spectrochim. Acta A Mol. Biomol. Spec.* **2013**, *112*, 132–138.

(36) Li, Z.; Lou, X.; Yu, H.; Li, Z.; Qin, J. An Imidazole-Functionalized Polyfluorene Derivative as Sensitive Fluorescent Probe for Metal Ions and Cyanide. *Macromolecules*, **2008**, *41*, 7433–7439.

(37) Özcan, E.; Tümay, S. O.; Alidağı, H. A.; Çoşut, B.; Yeşilot, S. A New Cyclotriphosphazene Appended Phenanthroline Derivative as A Highly Selective and Sensitive OFF–ON Fluorescent Chemosensor For Al^{3+} Ions. *Dyes Pigments*, **2016**, *132*, 230–236.

(38) Çetindere, S.; Tümay, S. O.; Kılıç, A.; Durmuş, M.; Yeşilot, S. Hexa-BODIPY Linked-Triazole Based on a Cyclotriphosphazene Core as a Highly Selective and Sensitive Fluorescent Sensor for Fe^{2+} Ions. *J. Fluores.* 2016, 26,1173–1181.

View Article Online
DOI: 10.1039/C7DT01134B

(39) Kağıt, R.; Yıldırım, M.; Ozay, O.; Yeşilot, S.; Ozay, H. Phosphazene Based Multicentered Naked-Eye Fluorescent Sensor with High Selectivity for Fe^{3+} Ions. *Inorg. Chem*. **2014**, *53*, 2144–2151.

(40) Ozay, H. Ozay, H. Yıldırım, M.; Yeşilot, S.; Ozay, O. Novel Hexapodal Triazole Linked to a Cyclophosphazene Core Rhodamine-Based Chemosensor for Selective Determination of Hg^{2+} Ions. *J. Fluores*. **2014**, *24*, 1593–1602.

(41) Çiftçi, G. Y.; Şenkuytu, E.; Durmuş, M., Yuksel, F.; Kılıç, A. Fluorenylidene Bridged Cyclotriphosphazenes: 'Turn-Off' Fluorescence Probe for Cu^{2+} and Fe^{3+} Ions. *Dalton Trans*. **2013**, *42*, 14916–14926.

(42) Wei, W.; Lu, R.; Tang, S.; Liu, X. Highly Cross-Linked Fluorescent Poly(Cyclotriphosphazene-Co-Curcumin) Microspheres for The Selective Detection of Picric Acid in Solution Phase. *J. Mater. Chem. A*, **2015**, *3*, 4604–4611.

(43) Şenkuytu, E.; Çiftçi, G. Y. Structural and Chemosensor Properties of FDA and FDP Derivatives of Fluorenylidene Bridged Cyclotetraphosphazenes. *Polyhedron*, **2016**, *115*, 247–256.

(44) Gleria, M.; De Jaeger R. (Eds.), Applicative Aspects of Cyclophosphazenes, Nova Science Publishers, Inc., New York, **2004**.

(45) Chandrasekhar, V.; Nagendran,S. Phosphazenes as Scaffolds for the Construction of Multi-Site Coordination Ligands. *Chem. Soc. Rev*. **2001**, *30*, 193–203.

(46) Ainscough, E. W.; Brodie, A. M.; Geoffrey, B. J.; Otter, C. A. Copper Complexes with 1,10-Phenanthrolines Tethered to a Cyclotriphosphazene Platform. *Polyhedron 2007*, *26*, 460–471.

(47) Chandrasekhar, V.; Thilagar, P.; Pandian, B. M. Cyclophosphazene-Based Multi-Site Coordination Ligands. *Coord. Chem.Rev*. **2007**, *251*, 1045–1074.

(48) Uslu, A.; Yeşilot, S. Chiral Configurations in Cyclophosphazene Chemistry. *Coord. Chem. Rev*. **2015**, *291*, 28–67.

(49) Gallicano, K. D.; Paddock, N. L. 1-Pyrazolyl Phosphazenes and Their Complexes with Palladium(II) Chloride and Platinum(II) Chloride. *Can. J. Chem*. **1982**, *60*, 521–528.

(50) Thomas, K. R. J.; Chandrasekhar, V.; Pal, P.; Scott, S. R.; Hallford, R.; Cordes, A. W. Unusual Tridentate N3 Capping Coordination Behavior of Hexakis(3,5-Dimethylpyrazolyl)Cyclotriphosphazene, N3P3(3,5-Me2Pz)6: Synthesis, Spectroscopy, and Electrochemistry of Mono- and Dinuclear Copper(II) Complexes and the X-Ray Structure of N3P3(3,5-Me2Pz)6.Cntdot.Cucl2. *Inorg. Chem*. **1993**, *32*, 606–611.

View Article Online
DOI: 10.1039/C7DT01134B

(51) Ainscough E. W.; Brodie, A. M.; Davidson, R. J.; Moubaraki, B.; Murray, K. S.; Otter, C. A.; Waterland, M. R. Metal-Metal Communication in Copper(II) Complexes of Cyclotetraphosphazene Ligands. *Inorg. Chem*. **2008**, *47*, 9182–9192.

(52) Ainscough, E. W.; Brodie, A. M.; Derwahl, A.; Kirk, S.; Otter, C. A. Conformationally Rigid Chelate Rings in Metal Complexes of Pyridyloxy-Substituted 2,2'-Dioxybiphenyl-Cyclotetra- and Cyclotriphosphazene Platforms. *Inorg. Chem.* **2007**, *46*, 9841–9852.

(53) Acock, K. G. Shaw, R. A. Wells, F. B. G. Phosphorus-Nitrogen Compounds. Part V. Friedel-Crafts Arylation of Hexachlorocyclotriphosphazatriene. *J. Chem. Soc*. **1964**, 121–130.

(54) Beşli, S.; Coles, S. J.; Davies, D. B.; Hursthouse, M. B. Kılıç, A.; Mayer, T. A.; Shaw, R. A.; Uslu, A. Structural investigations of phosphorus–nitrogen compounds. 4. Steric and electronic effects in dibenzylamino derivatives of hexachlorocyclotriphosphazatriene and 4,4,6,6-tetrachloro-2,2-diphenylcyclotriphosphazatriene. *Acta Crystallogr. Sect. B: Struct. Sci*. **2002**, *58*, 545–552.

(55) Chandrasekaran, A.; Krishnamurthy, S. S.; Nethaji, M. Palladium(II) Chloride Complexes of Bis(Pyrazolyl)Cyclotriphosphazenes. *Inorg.Chem*. **1993**, *32*, 6102–6106.

(56) Addison, A.W.; Rao, T. N.; Reedijk, J. J.; Rijn, V.; Verschoor, G. C. Synthesis, Structure, and Spectroscopic Properties of Copper(II) Compounds Containing Nitrogen–Sulphur Donor Ligands; The Crystal And Molecular Structure of Aqua[1,7- Bis(N-Methylbenzimidazol-2′-Yl)-2,6-Dithiaheptane]Copper(II) Perchlorate. *J. Chem. Soc*. *Dalton Trans*. **1984**, 1349–1356.

(57) Dobrzanska, L.; Kleinhans, D. J.; Barbour, L. J. Influence of The Metal-To-Ligand Ratio on the Formation of Metal Organic Complexes. *New J. Chem*. **2008**, *32*, 813–819.

(58) Richardson, C.; Steel, P. J. Benzotriazole as a Structural Component in Chelating and Bridging Heterocyclic Ligands; Ruthenium, Palladium, Copper And Silver Complexes. *Dalton Trans*, **2003**, 992–1000.

(59) Jeong, D. H. Park, W. J.; Jeong, J. H. Churchill, D. G.; Lee, H. Facile N–N Coupling and Copper (II) Promoted Cleavage of *N*,*N*′-Linked *N*-Methylbenzimidazole. *Inorg. Chem. Commun*. **2008**, *11*, 1170–1173.

(60) Liu, K.; Zhao, X.; Liu, Q.; Huo, J.; Zhu, B.; Diao, S. Fluoride-Driven 'Turn On' ESPT in the Binding with a Novel Benzimidazole-Based Sensor. *Beils. J. Org. Chem.* **2015**, 24, 563–567.

(61) Jayabharathi, J.; Thanikachalam, V.; Jayamoorthy, K. Synthesis of Some Fluorescent Benzimidazole Derivatives Using Cobalt(II) Hydroxide as Highly Efficient Catalyst–Spectral

View Article Online
DOI: 10.1039/C7DT01134B

and Physico-Chemical Studies and ESIPT Process. *Photochem. Photobiol. Sci*. **2013**, *12*, 1761–1773.

(62) Fakayode, S. O.; Busch, M. A.; Bellert, D. J.; Busch, K. W. Determination of the enantiomeric composition of phenylalanine samples by chemometric analysis of the fluorescence spectra of cyclodextrin guest–host complexes. *Analyst*, 2005, *130*, 233–241.

(63) Krishnamurthy, M.; Phaniraj, P. Dogra, S. K. Absorptiometric and fluorimetric study of solvent dependence and prototropism of benzimidazole homologues *J. CHEM. SOC. PERKIN TRANS. II* **1986**, 1917–1925.

(64) Hassan, A.; Habeeb, A.; Khalid, J.; Adilee, A.; Jaber, S. A. Thermal Decomposition Study on Solid Complexes of 7-[2-(Benzimidazolyl)azo]-8-hydroxy Quinoline with Co(III), Ni(II) and Cu(II). *Orient. J. Chem*. **2015**, *31*, 809–818.

(65) Paul, A.; Anbu, S.; Sharma, G.; Kuznetsov, M. L.; Guedes da Silva, M. F. C.; Koch, B.; Pombeiro, A. J. L. Intracellular Detection of Cu^{2+} And S^{2-} Ions Through a Quinazoline Functionalized Benzimidazole-Based New Fluorogenic Differential Chemosensor. *Dalton Trans*. **2015**, *44*, 16953–16964.

(66) Zheng, Y.; Orbulescu, J.; Ji, X.; Andreopoulos, F. M.; Pham, S. M.; Leblanc, R. M. Development of Fluorescent Film Sensors for the Detection of Divalent Copper. *J. Am. Chem. Soc*. **2003**, *125*, 2680–2686.

(67) Parker, C. A; Rees, W. Correction of Fluorescence Spectra and Measurement of Fluorescence Quantum Efficiency. *Analyst* **1960**, *85*, 587–600.

(68) Gabe, Y.; Urano, Y.; Kikuchi, K.; Kojima, H.; Nagano, T. Highly Sensitive Fluorescence Probes for Nitric Oxide Based on Boron Dipyrromethene Chromophore Rational Design of Potentially Useful Bioimaging Fluorescence Probe. *J. Am. Chem. Soc.* **2004**,*126*, 3357–3367.

(69) Liu, J.; Lu, Y. Rational Design of "Turn-On" Allosteric Dnazyme Catalytic Beacons for Aqueous Mercury Ions with Ultrahigh Sensitivity and Selectivity. *Angew. Chem.* **2007**, *119*, 7731–7734.

(70) Bruker, SADABS, Bruker AXS Inc., Madison, Wisconsin, USA, **2005**

(71) Bruker *APEX2* (Version 2011.4-1) Bruker AXS Inc., Madison, Wisconsin, USA, **2008**

(72) Sheldrick, G. M. SHELXS97. Programs for crystal structure solution.

(73) A. L. Spek, *J. Appl. Crystallogr.*, **2003**, *36*, 7–13.

(74) Macrae, C. F.; Edgington, P. R.; McCabe, P.; Pidcock, E.; Shields, G. P.; Taylor, R.; Towler, M.; van de Streek, J. *J. Appl. Cryst.* **2006**, *39*, 453–457.

View Article Online
DOI: 10.1039/C7DT01134B

(75) Brandenburg, K. DIAMOND 3.1 for Windows. Crystal Impact GbR, Bonn, Germany, **2006**.

(76) Becke, A. D. *J. Chem. Phys*. **1993**, *98*, 5648–5652.

(77) Lee, C.; Yang, W.; Parr, R. G. *Phys. Rev. B* **1988**, *37*, 785–789.

(78) Hehre, W. J.; Rado, L.; Scheleyer, P.V.R.; Pople, J. A. Ab initio Molecular Orbital Theory, Wiley, New York, **1986**.

(79) Frisch, M. J.; Trucks, G. W. ; Schlegel, H. B. ; Scuseria, G. E. ; Robb, M. A. ; Cheeseman, J. R. ; Scalmani, G.; Barone, V. ; Mennucci, B.; Petersson, G. A.; Nakatsuji, H.; Caricato, M.; Li, X.; Hratchian, H. P.; Izmaylov, A. F.; Bloino, J.; Zheng, G.; Sonnenberg, J. L.; Hada, M.; Ehara, M.; Toyota, K.; Fukuda, R.; Hasegawa, J.; Ishida, M.; Nakajima, T.; Honda, Y.; Kitao, O.; Nakai, H.; Vreven, T.; Montgomery, J. A.; Peralta, Jr. J. E.; Ogliaro, F.; Bearpark, M.; Heyd, J. J.; Brothers, E.; Kudin, K. N.; Staroverov, V. N.; Kobayashi, R.; Normand, J.; Raghavachari, K.; Rendell, A.; Burant, J. C.; Iyengar, S. S.; Tomasi, J.; Cossi, M.; Rega, N.; Millam, J. M.; Klene, M.; Knox, J. E.; Cross, J. B.; Bakken, V.; Adamo, C.; Jaramillo, J.; Gomperts, R.; Stratmann, R. E.; Yazyev, O.; Austin, A. J.; Cammi, R.; Pomelli, C.; Ochterski, J. W.; Martin, R. L.; Morokuma, K.; Zakrzewski, V. G.; Voth, G. A.; Salvador, P.; Dannenberg, J. J.; Dapprich, S.; Daniels, A. D.; Farkas, O.; Foresman, J. B.; Ortiz, J. V.; Cioslowski, J.; Fox, D. J.; Gaussian, Inc., Wallingford CT, **2009**.

View Article Online
DOI: 10.1039/C7DT01134B

We present a comprehensive work that fluoroprobe properties of synthesized compounds for copper ion detection were discussed with a stereochemical approach and using X-ray crystallographic analysis results for the sensing mechanism.